

THE EFFECT OF CATION SUBSTITUTIONS
ON THE PHYSICAL PROPERTIES
OF TRIOCTAHEDRAL MICAS

by

Robert Miller Hazen

SUBMITTED IN PARTIAL FULFILLMENT
OF THE REQUIREMENTS FOR THE
DEGREE OF MASTER OF
SCIENCE
at the
MASSACHUSETTS INSTITUTE OF
TECHNOLOGY

June, 1971

Signature of Author
Department of Earth and Planetary Sciences,
May 8, 1971

Certified by Thesis Supervisor

Accepted by Chairman, Departmental Committee
Lindgren on Graduate Students



ABSTRACT

-2-

The Effect of Cation Substitutions on the
Physical Properties of trioctahedral Micas

by

Robert Miller Hazen

Submitted to the Department of Earth and Planetary Sciences
in partial fulfillment of the requirement for the
degree of Master of Science
June, 1971

Unit cell dimensions and refractive indices have been determined for synthetic hydrous trioctahedral micas in which each of Co^{+2} , Cu^{+2} , Fe^{+2} and Ni^{+2} completely occupies the octahedral sites. Zn and Mn micas with excess aluminum have also been synthesized, but syntheses of pure Zn^{+2} , Mn^{+2} , Cd^{+2} and Pb^{+2} micas were not successful. Tetrahedral substitutions of B^{+3} , Fe^{+3} and Ga^{+3} for Al^{+3} and Ge^{+4} for Si^{+4} ; and interlayer cation substitutions of Rb^+ , Cs^+ , NH_4^+ and Na^+ for K^+ provide additional data on linear relationships that exist between ionic radii (Shannon and Prewitt) and unit cell edges, and between ionic radii cubed and unit cell volumes of these micas. The influence of substitutions on the unit cell are such that octahedral substitutions predominantly affect the a-dimension, interlayer substitutions the c-dimension, and tetrahedral substitutions affect both dimensions.

Tetrahedral and interlayer cation substitutions of a wide range of ionic radii were found to form stable micas. However, octahedral cations of greater than 0.78 \AA average ionic radius do not form stable trioctahedral micas of the form $\text{KR}_3^{+2}\text{AlSi}_3\text{O}_{10}(\text{OH})_2$. The instability of such micas is shown to be due to the misfit of smaller tetrahedral layers onto a larger octahedral layer. The composition of natural biotites are explained on the basis of this model. In addition, quantitative predictions of the amount of Fe^{+3} in octahedral and tetrahedral positions in synthetic annite were made, and have been confirmed by Mössbauer and analytical chemistry techniques. A nomogram is constructed in which, for any given composition of a hydrous trioctahedral mica, the relative stability of the mica may be determined.

Thesis Supervisor: David R. Wones
Title: Associate Professor of Geology

TABLE OF CONTENTS

-3-

TITLE PAGE	1
ABSTRACT	2
TABLE OF CONTENTS	3
ACKNOWLEDGMENTS	5
INTRODUCTION	6
Table 1--Previous studies	7
MICA COMPOSITIONS STUDIED	8
EXPERIMENTAL TECHNIQUE	9
Table 2--Chemicals Used	11
Table 3--Mica Synthesis Experiments	14
UNIT CELL PARAMETERS	20
Table 4--Unit Cell Parameters of Synthetic Micas	21
OPTICAL DATA	23
Table 5--Optical Properties of Synthetic Micas	25
SOURCES OF ERROR	26
RELATIONS BETWEEN CELL PARAMETERS AND IONIC RADII	29
Figure 1--Monoclinic b_m vs. octahedral cation radius--	31
Figure 2-- c_m vs. interlayer cation radius	33
Figure 3--Volume vs. ionic radii cubed for R^{+2}	35
Figure 4--Volume vs. ionic radii cubed for R^+ and R^{+3-}	37
Figure 5-- d_{001} vs. b_m	39
SUBSTITUTIONS AND STABILITY	41
Figure 6--Octahedral layer compression	43
Figure 7-- Ψ vs. ionic radius R^{+2}	46
Figure 8--Tetrahedral layer rotation	48
Figure 9-- α vs. ionic radius R^{+2}	51

OCTAHEDRAL CATION DISTRIBUTION IN NATURAL MICAS	53
Figure 10-- R^{+2} composition in natural micas	54
THE COMPOSITION OF ANNITE	56
PREDICTION OF TRIOCTAHEDRAL MICA STABILITY	58
Figure 11-- α vs. cation radius R^{+2}	59
Figure 12--Nomogram of $\cos\alpha$ vs. ionic radii vs. d_t	61
FUTURE STUDIES	63
REFERENCES	65
APPENDIX A--The Stability of Hydrous Trioctahedral Micas and their Related Hydroxides	70
Introduction	70
Experiments and Data	71
Preliminary Conclusions	71
Table A-1--Stability experiments	72
Table A-2--Cell Parameters of oxides and hydroxides	74
APPENDIX B--Selected Computer d-spacings for synthetic Micas	76
VITA	87

ACKNOWLEDGMENTS

I wish to express my great appreciation to Prof. David R. Wones for his many hours of advice and guidance. Not only did he provide the initial outline for this study, but he also maintained close contact as the study progressed, thus adding direction and enthusiasm to my efforts.

I would also like to thank Messrs Robert Charles, Joseph Chernosky , Yves Pelletier, and Dr. David Hewitt for aiding me in many aspects of laboratory techniques and maintenance. Many hours of labor were saved through their suggestions and aid.

Many thanks are also due to Prof. Charles W. Burnham, Prof. Charles T. Prewitt, Dr. Hiroshi Takeda, and Dr. James Munoz for their stimulating discussions and many helpful comments.

This investigation was supported by National Science Foundation grants GA1109 and GA13092 to Prof. David R. Wones.

Introduction

Trioctahedral micas are subject to a wide variety of cation substitutions. Several authors have demonstrated that such substitutions have a profound effect on both the physical properties and the stabilities of these layer silicates (Hatch et al., 1957; Wones, 1963b; Klingsberg and Roy, 1957). A list of several recent studies on synthetic hydrous trioctahedral micas is given in Table One. While data is now available for a dozen such mica end-members, there has been little attempt to systematically examine changes in mica properties with composition. The present study is an attempt to quantitatively define the effects of a wide range of cation substitutions on the physical properties of hydrous trioctahedral micas.

TABLE I. Previous Studies of Synthetic Hydrous Trioctahedral Micas

<u>Composition</u>	<u>Emphases of Study</u>	<u>References</u>
$KMg_3AlSi_3O_{10}(OH)_2$	Physical Properties & Stability Stability Structure	Yoder & Eugster (1954) Wones (1967) Steinfink (1962)
$KFe_3AlSi_3O_{10}(OH)_2$	Stability & Physical Properties Stability & Physical Properties	Eugster & Wones (1962) Wones, Burns & Carroll (1971)
$K(Mg,Fe)_3AlSi_3O_{10}(OH)_2$	Physical Properties Stability	Wones (1963) Wones & Eugster (1965)
$KMg_3FeSi_3O_{10}(OH)_2$	Physical Properties	Wise & Eugster (1964)
$KFe_3FeSi_3O_{10}(OH)_2$	Physical Properties	Wones (1963a)
$KMg_3BSi_3O_{10}(OH)_2$	Physical Properties Physical Properties	Eugster & Wright (1960) Stubicon & Roy (1962)
$KMg_3GaSi_3O_{10}(OH)_2$	Stabilities only	Klingsberg & Roy (1957)
$KNi_3AlSi_3O_{10}(OH)_2$		DeVries & Roy (1958)
$KZn_3AlSi_3O_{10}(OH)_2$	Unit Cell Parameters	Frondel & Ito (1966)
$KMn_3AlSi_3O_{10}(OH)_2$		
$NaMg_3AlSi_3O_{10}(OH)_2$	Physical Properties	Carman (1969)
$NH_4Mg_3AlSi_3O_{10}(OH)_2$	Physical Properties	Eugster & Munoz (1966)

Mica Compositions Studied

The hydrous magnesian trioctahedral mica, phlogopite, $KMg_3AlSi_3O_{10}(OH)_2$, was used as the reference composition in this study. Attempted 100% octahedral substitutions for Mg^{+2} included Mn^{+2} , Co^{+2} , Ni^{+2} , Cu^{+2} , Zn^{+2} , Cd^{+2} , and Pb^{+2} . Data of Wones (1963b) on the Fe^{+2} mica annite, and synthetic biotites on the join phlogopite-annite, have also been employed. Tetrahedral cation substitutions were Ga^{+3} , Fe^{+3} , and B^{+3} for Al^{+3} , and Ge^{+4} for Si^{+4} ; while substitutions into the interlayer cation K^+ position include Rb^+ , Cs^+ , Cu^+ , and Ag^+ . In addition, Na^+ phlogopite data of Carman (1969) and NH_4^+ phlogopite data of Eugster and Munoz (1966) have been used in this study. Finally, a number of double 100% cation substitutions into the phlogopite structure were studied, including ferriannite- $KFe_3^{+2}Fe^{+3}Si_3O_{10}(OH)_2$ (data of Wones, 1963a), nickelous ferriphlogopite- $KNi_3FeSi_3O_{20}(OH)_2$, cobaltous ferriphlogopite- $KCo_3FeSi_3O_{10}(OH)_2$ and sodium-zinc phlogopite- $NaZn_3AlSi_3O_{10}(OH)_2$.

Experimental Technique

A complete list of chemicals and their lot numbers used in starting material preparation will be found in Table Two. Cobaltous hydroxide was prepared by the T.A. Edison precipitation method (U.S. Patent # 1,167,484) in which ammonium hydroxide is added to a cobaltous sulfate solution. The precipitate of $\text{Co}(\text{OH})_2$ is washed five times in deionized and distilled water, and then dried at 100°C for 4h. γ -alumina was prepared by heating $\text{AlCl}_3 \cdot 6\text{H}_2\text{O}$ for 1h. at 750°C. The silicate glass was cleaned both magnetically and in acid, and fired at 800°C for 2h. before using. $\text{K}_2\text{O} \cdot 2\text{SiO}_2$ was prepared by D.R. Wones from cleaned SiO_2 glass and KHCO_3 , after the method of Schairer and Bowen (1955). Starting materials of five types were used:

- 1) Oxide Mix
- 2) $\text{K}_2\text{Si}_2\text{O}_5$ plus oxides
- 3) KAlSi_3O_8 gel plus R^{+2} oxide or hydroxide
- 4) KFeSi_3O_8 gel plus R^{+2} oxide or hydroxide
- 5) Mica gel

All gels were prepared by titration of standardized nitrate solutions. The solution mixes were dried and fired as described by Shaw (1963). Oxide mixes were prepared by weighing and mixing dried oxides or hydroxides, and then grinding in an agate mortar until homogeneous.

Charges were sealed with excess deionized and distilled water, or 30% H_2O_2 solution in Au or Ag₈₀Pd₂₀ 1/8" x 1/2"

capsules. In several runs oxygen fugacities were controlled by the solid buffer technique of Eugster (1957). Standard cold seal hydrothermal pressure apparatus was used in all runs (Tuttle, 1949). Pressure measurements are believed accurate within 1%, and the error in temperature is within $\pm 3^{\circ}\text{C}$. All runs were rapidly quenched (2 minutes) in a cool water bath.

X-ray powder diffraction examination of all runs was performed on a Picker diffractometer using Cu K_{α} radiation, and data was collected on a servoriter strip chart recorder. Both CaF_2 (Baker's Analytical Reagent lot #91548; annealed 3X at 800°C for 1h.; $a = 5.4620 \pm .0005$) and BaF_2 (Baker's lot #308; annealed 2X at 800°C for 1h.; $a = 6.1971 \pm .0002$) were employed as internal standards. Least squares unit cell refinements were performed on the Appleman, Handworker and Evans program. Optical data was obtained using a Zeiss binocular polarizing microscope with a white light source. Determination of mica indices of refraction were accomplished with Cargille's Index of Refraction Liquids, which are accurate to within $\pm .0005$. All x-ray diffraction and optical work was performed at room temperature ($24^{\circ} \pm 1^{\circ}\text{C}$).

TABLE 2. Chemicals used in starting material preparation

Chemicals used in oxide mix preparation

<u>Formulae</u>	<u>Manufacturer (& Grade)*</u>	<u>Lot Number</u>
SiO ₂ glass	Corning (lump cullet)	7940
GeO ₂ (trigonal)	Fisher	786604
AlCl ₃ · 6H ₂ O	Mallinkrodt	15961X
Fe ₂ O ₃	Fisher	762942
B ₂ O ₃	J.T. Baker	39315
MgO	Fisher	787699
MnO	K & K	10868
CoSO ₄ · 7H ₂ O	Mallinkrodt	n.d.
NiO	Matheson, Coleman & Bell	CB918 NX345
CuO	Mallinkrodt	X40588
ZnO	Baker & Adamson	B354
CdO	Baker & Adamson	A244X364J
Ni(OH) ₂	K & K	16214
NH ₄ (OH)	J.T. Baker	24037
KHCO ₃	J.T. Baker	21537

TABLE 2. Continued

<u>Formulae</u>	<u>Manufacturer (& Grade)*</u>	<u>Lot Number</u>
K(OH)	J.T. Baker	14890
Ag ₂ O	K & K	17692
Cu ₂ O	Fisher	n.d.

Additional chemicals used in gel preparations

"Ludox"**	Dupont (High Silica)	n.d.
Ag Metal	Fisher	71096
Cu Metal	Baker & Adamson	N-023
Zn Metal	Merck	40678
Pb Metal	Fisher (8/1000" foil)	n.d.
Ga Metal	J.T. Baker (99.999%)	n.d.
KNO ₃	J.T. Baker	30158
NaNO ₃	J.T. Baker	33275
RbNO ₃	K & K	18088
CsNO ₃	K & K	7824

TABLE 2. Continued

<u>Formuale</u>	<u>Manufacturer (& Grade)*</u>	<u>Lot Number</u>
Mg (NO ₃) ₂ · 6H ₂ O	Mallinkrodt	37012
Mn (NO ₃) ₂	Mallinkrodt (50% solution)	27357
Al (NO ₃) ₃ · 9H ₂ O	Mallinkrodt	26829
Cr (NO ₃) ₃ · 9H ₂ O	Mallinkrodt	795204

*All chemicals reagent grade unless noted.

**Dupont Ludox was analyzed by F. Frey. Solids after drying and firing at 300°C include by weight SiO₂ = 99.0% and Na₂O = 1.0%.

TABLE 3. Mica Synthesis Experiments

Micas of the form $R^+Mg_3AlSiO_{10}(OH)_2$

<u>R⁺ cation</u>	<u>R⁺ ionic radius (Å)</u>	<u>Run #</u>	<u>P_T = P_{H₂O} (in kbars)</u>	<u>T (°C) (± 3°)</u>	<u>Duration (hours)</u>	<u>Starting Materials</u>	<u>Capsule Buffer</u>	<u>Products</u>
K ⁺	1.38	M#1	2.0	800	70	gel	Au	100% phlogopite
Rb ⁺	1.49	M#105	2.0	700	140	gel	Au	Rb-phlogopite, Forsterite, & RbAlSi ₂ O ₆
		M#98	2.0	300	340	gel	Au	do. plus glass
Cs ⁺	1.70	M#106	2.0	700	140	gel	Au	Cs-Phlogopite, Forsterite, & CsAlSi ₂ O ₆
		M#99	2.0	300	340	gel	Au	Forsterite, CsAlSi ₂ O ₆ & glass
Ag ⁺	1.15	M#46	2.0	310	48	gel	Au	Silver Metal & glass
		M#67	2.0	540	48	gel	Pt	do.
		M#90	2.0	600	72	Mg ₃ AlSi ₃ gel plus Ag ₂ O	Au	Silver Metal, Chlorite & glass
Cu ⁺	0.96	M#122	2.0	630	96	Oxide Mix	Au	Cu ₂ O, Talc & unknown

TABLE 3. Continued

Micas of the form $KR_3^{+2}AlSi_3O_{10}(OH)_2$

<u>R⁺ cation</u>	<u>R⁺ ionic radius (A.)</u>	<u>Run #</u>	<u>P_T = P_{H₂O} (in kbars)</u>	<u>T (°C) (3°)</u>	<u>Duration (hours)</u>	<u>Starting Materials</u>	<u>Capsule Buffer</u>	<u>Products</u>
Mg ⁺²	0.720	M#1	2.0	800	70	gel	Au	100% Phlogopite
Mn ⁺²	0.83	M#13	2.0	450	96	Oxide Mix & K ₂ Si ₂ O ₅ gel	Au	α -Mn ₂ O ₃ ; γ -Mn ₂ O ₃ & sanidine
		M#18	2.0	280	216	Reduced Oxide Mix	Au	MnO; Mn(OH) ₂ & glass
		M#19	2.0	362	120	Reduced Oxide Mix	Au	Tephroite, Kalsitite & Leucite
		M#32	2.0	603	120	Gel	Au	Mn(OH) ₂ & Manganophyllite
		M#62	2.0	725	72	Gel	Au	γ -Mn ₂ O ₃ & Sanidine
		M#86	2.0	540	96	Reduced Gel	Au	Braunite, Tephroite Sanidine & <10% Mica
		M#84	2.0	580	670	Reduced Gel	Au	Braunite & Sanidine
		M#91	1.0 kb CH ₄	500	336	M#32	Ag-Pd	Mn(OH) ₂ & Manganophyllite
		M#92	1.0 kb CH ₄	500	336	Gel	Ag-Pd	Tephroite, Kalsilite & Leucite
		M#117	1.0 kb CH ₄	600	96	MnO plus Kfs gel	Ag-Pd	Tephroite, Kalsilite & Leucite

TABLE 3. Continued

<u>R+2 cation</u>	<u>R+2 ionic radius (A°)</u>	<u>Run #</u>	<u>P_T = P_{H₂O} (in kbars)</u>	<u>T (°C) (±3°)</u>	<u>duration (hours)</u>	<u>Starting Materials</u>	<u>Capsule Buffer</u>	<u>Products</u>
Co^{+2}	0.745	M#114	2.0	750	48	Co(OH)_2 plus gel	Au	100% Cobaltous Phlogopite
		SR#12	1.0	710	48	Co(OH)_2 plus gel	Au	100% Cobaltous Phlogopite
		SR#34	0.2	880	48	SR#12	Au	CoO, Co Olivine & Leucite
Ni^{+2}	0.69	M#7b	2.0	600	145	Oxide mix plus $\text{K}_2\text{Si}_2\text{O}_5$ gel	Au	100% Nickelous Phlogopite
		M#115	2.0	750	48	Ni(OH)_2 plus Au gel	Au	100% Nickelous Phlogopite
Cu^{+2}	0.73	M#29	2.0	600	120	Gel	Au	80% Cupric Phlogopite, glass and minor unidentified ♀
		M#49	2.0	703	96	Gel	Au	50% Cupric Phlogopite, glass and unidentified phase
		M#77	2.0	260	215	Gel	Au	Cupric Phlogopite, Cu-Pyroxene & Muscovite

TABLE 3. Continued

<u>R⁺² cation</u>	<u>R⁺² ionic radius (Å)</u>	<u>Run #</u>	<u>P_T = P_{H₂O} (in kbars)</u>	<u>T (°C) (±3°)</u>	<u>Duration (hours)</u>	<u>Starting Materials</u>	<u>Capsule Buffer</u>	<u>Products</u>
Zn^{+2}	0.75	M#8	2.0	600	145	Oxide mix & $K_2Si_2O_5$	Au	Willemite, Kalsilite & Leucite
		M#17	2.0	280	215	Oxide mix & $K_2Si_2O_5$	Au	Willemite, Mica & minor Leucite
		M#61	2.0	725	72	Gel	Au	Willemite, Kalsilite & Leucite
		M#94	2.0	530	50	Gel	Au	Willemite, Mica & Leucite
		M#101	2.0	500	290	Gel	Au	Willemite, Mica & Leucite
Cd^{+2}	0.95	M#9	2.0	600	145	Oxide mix & $K_2Si_2O_5$	Au	Cd-Olivine & Leucite
		M#22	2.0	385	360	Reduced Oxide mix	Au	Cd-Olivine & Sanidine
Pb^{+2}	1.18	M#57	2.0	650	290	Gel	Au	Pb_4SiO_6 & unknown
		M#66	2.0	410	170	Gel	Au	$K_2Pb_4Si_8O_{21}$, Sanidine & Pb_3O_4

Table 3. Continued

<u>R⁺³ cation</u>	<u>R⁺³ ionic radius (Å)</u>	<u>Run #</u>	<u>P_T = P_{H₂O} (in kbars)</u>	<u>T (°C) (±3°)</u>	<u>Duration (hours)</u>	<u>Starting Materials</u>	<u>Capsule Buffer</u>	<u>Products</u>
Micas of the form KMg ₃ R ⁺³ Si ₃ O ₁₀ (OH) ₂								
Al ⁺³	0.39	M#1	2.0	800	70	Gel	Au	100% Phlogopite
B ⁺³	0.12	M#30	2.0	603	120	Oxide Mix & K ₂ Si ₂ O ₅	Au	50% Boron Phlogopite, Glass
		M#108	2.0	720	120	Oxide Mix & K ₂ Si ₂ O ₅	Au	95% Boron Phlogopite
Ga ⁺³	0.47	M#46	2.0	310	45	Gel	Au	40% Gallium, Phlogopite Ga ₂ O ₃ , unknown ♀, & glass
		M#109	2.0	720	120	Gel	Au	100% Gallium Phlogopite
Fe ⁺³	0.49	M#100	2.0	500	265	Oxide Mix & K ₂ SiO ₅	Au	100% Ferri-Phlogopite
		M#107	2.0	720	120	Oxide Mix & K ₂ Si ₂ O ₅	Au	100% Ferri-Phlogopite
Cr ⁺³ (IV)	n.d.	M#111	2.0	690	215	Oxide Mix & K ₂ Si ₂ O ₅	Au	100% Ferri-Phlogopite
		M#44	2.0	700	96	Gel	Au	Cr ₂ O ₃ , Forsterite & unknown ♀
		M#72	2.0	410	31	Gel	Au	Cr ₂ O ₃ , Forsterite & glass

TABLE 3. Continued

<u>R⁺⁴ cation</u>	<u>R⁺⁴ ionic radius (A°)</u>	<u>Run #</u>	<u>P_T = P_{H₂O} (in kbars)</u>	<u>T (°C) (± 3°)</u>	<u>Duration (hours)</u>	<u>Starting Materials</u>	<u>Capsule Buffer</u>	<u>Products</u>
Micas of the form KMg ₃ AlR ₃ ⁺⁴ O ₁₀ (OH) ₂								
Si ⁺⁴	0.26	M#1	2.0	800	70	Gel	Au	100% Phlogopite
Ge ⁺⁴	0.40	M#63	2.0	725	75	Oxide Mix	Au	100% Ge-Phlogopite
Micas of the form KR ₃ ⁺² FeSi ₃ O ₁₀ (OH) ₂								
Mg ⁺²	0.72	M#100	2.0	500	265	Oxide Mix & K ₂ Si ₂ O ₅	Au	100% Ferri-phlogopite
		M#107	2.0	720	120	Oxide Mix & K ₂ Si ₂ O ₅	Au	100% Ferri-phlogopite
		M#111	2.0	690	215	Oxide Mix & K ₂ Si ₂ O ₅	Au	100% Ferri-phlogopite
Ni ⁺²	0.69	M#123	2.0	700	24	Ni(OH) ₂ & KFeSi ₃ O ₈ Gel	Au	100% Nickelous Ferri-phlogopite
Co ⁺²	0.745	M#127	2.0	700	24	Co(OH) ₂ & KFeSi ₃ O ₈ Gel	Au	100% Cobaltous Ferri-phlogopite

Unit Cell Parameters

1M unit cell dimensions and volumes, as well as molecular weights and calculated densities, for synthetic hydrous trioctahedral micas of this and other studies are listed in Table Four. Smith and Yoder (1956) have shown that trioctahedral micas often possess an ideal pseudo-trigonal unit cell, defined by $a_m = b_m/\sqrt{3}$ and $\beta_m = 99^\circ 54'$. The conversion from the monoclinic 1M to trigonal 3T cell is accomplished by $a_t = a_m$ and $c_t = 3c_m \cdot \sin\beta_m$. Of the micas examined, only sodium and boron phlogopites depart appreciably from these ideal relations.

Crowley and Roy (1960) have demonstrated that pressure of formation does not significantly affect unit cell parameters of phlogopite. Similarly, synthetic micas examined in this study showed no systematic variations of cell parameters with temperature or pressure. However, Eugster and Wright (1966) have noted that the physical properties of boron phlogopite appear to vary with temperature and pressure of formation. Also, Carman (1969) has clearly documented the tendency of sodium phlogopite to hydrate below 80°C. Thus, sodium and boron phlogopite once again depart from the ideal case. It should be noted that sodium and boron phlogopites have the smallest cell dimensions of all micas studied.

TABLE 4. Unit Cell Parameters of Synthetic Hydrous Trioctahedral Micas

Micas of Known Composition								
<u>Composition</u>	<u>a_m (Å°)</u>	<u>b_m (Å°)</u>	<u>c_m (Å°)</u>	<u>f_m</u>	<u>Vol (Å°)³</u>	<u>GFW</u>	<u>ρ_{calc} g/cm³</u>	<u>Run# or Reference</u>
<u>KMg₃AlSi₃O₁₀(OH)₂</u>	5.315±.001	9.204±.002	10.311±.003	99°54'±4'	497.0±0.6	417.3	2.79	M#1
	5.314±.001	9.208±.002	10.314±.005	99°54'±2'	497.0±1.0			Wones (1966)
	5.314±.01	9.204±.02	10.314±.005	99°54'±5'	497.0±1.0			Yoder & Eugster (1954)
<u>Na⁺Mg₃AlSi₃O₁₀(OH)₂</u>	5.265±.008	9.203±.006	9.994±.001	97°45'±8	479.8±0.8	401.2	2.78	Carman (1969) 1
<u>NH₄⁺</u>	5.311±.008	9.224±.004	10.443±.007	99°42'	504.2	396.2	2.61	Eugster & Munoz (1966)
<u>Rb⁺</u>	5.34 ±.01	9.24 ±.02	10.48 ±.05	99°54'	510.0	463.6	3.02	M#105 2
<u>Cs⁺</u>	5.37 ±.01	9.30 ±.02	10.83 ±.05	99°54'	516.8	510.8	3.18	M#106 2
<u>KCo⁺²AlSi₃O₁₀(OH)₂</u>	5.340±.001	9.240±.005	10.345±.002	99°58'±2	502.8±0.3	521.1	3.44	M#114
	5.341±.001	9.240±.002	10.347±.002	99°54'	503.3			SR#12 2
	5.303±.005	9.172±.001	10.286±.002	99°56'±3'	493.1±.5			M#7b
<u>Ni₃⁺²</u>	5.297±.003	9.175±.003	10.281±.004	99°50'±3'	492.3±.3	520.5	3.51	M#115
	n.d.	n.d.	10.17	n.d.	n.d.			Klingsberg & Roy (1957)
	5.334±.001	9.238±.002	10.314±.004	99°54'	498.8±.4	535.0	3.56	M#29 2
<u>Cu₃⁺²</u>	5.330±.001	9.234±.002	10.316±.003	99°56'±2'	497.8±.2			M#49
	5.401±.01	9.347±.005	10.297±.01	100°10'±12'	511.7	511.9	3.32	Wones (1963b)
	5.397±.001	9.348±.002	10.316±.005	99°54'±	512.0			Wones, Burns & Carroll (1971) 2
<u>(FeMg)₃-Mole % Fe 0.169</u>	5.339±.006	9.230±.001	10.311±.002	99°50'±4'	500.6			Wones (1963b)
	0.250	5.333±.002	9.242±.001	10.312±.001	99°56'±1'	500.6		
	0.352	5.349±.005	9.260±.002	10.293±.006	99°38'±6'	502.6		
	0.450	5.343±.007	9.276±.001	10.312±.003	99°57'±4'	503.4		
	0.550	5.358±.003	9.285±.003	10.297±.002	100°0' ±1'	504.5		
	0.765	5.373±.01	9.312±.003	10.297±.009	100°3' ±6'	507.3		
	0.880	5.389±.003	9.335±.002	10.322±.004	99°58'±4'	511.4		

TABLE 4. Continued

<u>Composition</u>	<u>a_m (Å°)</u>	<u>b_m (Å°)</u>	<u>c_m (Å°)</u>	<u>β_m</u>	<u>Vol (Å°)³</u>	<u>GFW</u>	<u>ρ_{calc} gm/cm³</u>	<u>Run # or Reference</u>
KMg ₃ B ⁺³ Si ₃ O ₁₀ (OH) ₂	5.29±.002	9.177±.001	10.246±.002	98°34'±4'	491.9±.2	401.1	2.77	M#108
	5.32±.01	9.165±.02	10.29 ±.01	100°10'±10'	496.5			Eugster & Wright (1960)
	5.310	9.150	10.234	100° 8'	489.5			Stubicon & Roy (1962)
G ₃ ⁺³	5.327±.002	9.218±.005	10.359±.002	99°49'±2'	501.2±.3	460.0	3.05	M#109
	n.d.	n.d.	10.26	n.d.	n.d.			Klingsberg & Roy (1957)
Fe ₃ ⁺³	5.354±.001	9.273±.002	10.316±.004	99°54'	505.0±.2	446.1	2.93	M#107 2
	5.358±.003	9.276±.003	10.321±.004	99°58'±4'	505.2±.3			M#111 3
	5.34 ±.01	9.28 ±.005	10.35 ±.01	99°55'±10'	505.6			Wise & Eugster (1964)
KMg ₃ AlGe ⁺⁴ O ₁₀ (OH) ₂	5.393±.002	9.341±.004	10.600±.002	99°54'	526.1±1.0	550.8	3.48	M#63 2
	5.387±.002	9.378±.02	10.593±.003	99°43'±2'	525.5±1.0	550.8		M#68
KFe ₃ ⁺² Fe ⁺³ Si ₃ O ₁₀ (OH) ₂	5.430±.002	9.404±.005	10.341±.006	100°4'±10'	519.9	540.76	3.45	Wones (1963a)
KNi ₃ Fe ⁺³ i ₃ O ₁₀ (OH) ₂	5.335±.005	9.237±.005	10.332±.006	99°55'±10'	501.5±.08	549.34	3.63	M#123
KCo ₃ Fe ⁺³ Si ₃ O ₁₀ (OH) ₂	5.368±.001	9.329±.002	10.346±.002	99°50'±5'	510.1±.04	550.00	3.58	M#127

Synthetic Micas of Unknown Composition

<u>R⁺² Cation & Extra Phases</u>						
Zn ⁺²	5.31±.02	9.205±.01	10.25± .05	99°50'±10'	492.5±1.0	M#17
Willemite 25% in all runs	5.303±.004	9.214±.005	10.285±.003	99°41'±3'	495.4±.4	M#94
	5.328±.002	9.226±.002	10.312±.004	99°59'±1'	498.9±.2	M#101
Willenite reported from all runs	5.325±.005	9.210±.005	10.210	99°50'±10'	493.0±1.0	Frondel & Ito (1966) ⁴
Mn ⁺²	5.27±.01	9.20±.02	10.17±.03	99°50'±10'		M#32
Mn(CH) ₂ 25% in all runs	5.31±.01	9.21±.01	10.31±.01	99°45'±6'	503±3	M#91
Tephroite reported in all runs	5.32±.01	9.394±.01	10.32±.01	99°50'±10'		Frondel & Ito (1966) ⁴

1. X-ray diffraction performed at 130°C.
2. 1M unit cell calculated from ideal 3T cell data.
 $a_m = a_t$, $b_m = \sqrt{3} \cdot a_t$, $c_m = ct/3 \cdot \sin 99°54'$, $\beta_m = 99°54'$
3. Mössbauer analyses of ferriphlogopites by R. Burns reveals 5 to 15% Fe⁺² in all runs.
4. Unit cell parameters calculated on the Appleman, Handworker & Evans Program by this author from Frondel & Ito (1966), Table 7, p. 1421.

Optical Data

Indices of refraction for synthetic hydrous trioctahedral micas of this and other studies are found in Table Five. Due to the psuedo-trigonal habit of these micas, $\gamma \approx \beta$, and thus two refractive indices are definitive. Other optical parameters considered include birefringence $B = \gamma - \alpha$ and the observed mean refractive index $\bar{n} = \sqrt[3]{\alpha \cdot \gamma^2} \approx \frac{2\gamma + \alpha}{3}$. While synthetic crystallites seldom exceeded 20μ in size, thus making $2V$ determination difficult, all observed $2V \approx 0^\circ$. Micas are colorless except for those containing cations of the transition metal series. Intense pleochroism was observed only in iron-bearing trioctahedral micas, whereas faint pleochroism was noted in cobalt and copper phlogopites.

A useful, but seldom used optical property is the specific refractive energy K , defined by $K = \bar{n} - 1/\rho$ where \bar{n} is the mean refractive index and ρ the density. Gladstone and Dale (1864) demonstrated that K for liquids may be calculated from the formula: $K = k_1 (P_1/100) + k_2 (P_2/100) + \text{etc.}$, where k_1 , k_2 , etc. are the specific refractive energies of the components of the liquids and P_1 , P_2 , etc. are the weight percentages of these components. H.W. Jaffe (1956) applied the rule of Gladstone and Dale to minerals, treating oxides as the components of the minerals. Jaffe obtained reasonable agreement between observed and calculated \bar{n} in this manner. However, it is interesting to note that the calculated \bar{n} for hydrous silicates displayed consistent positive deviations from those considered in Jaffe's study.

observed \bar{n} . Deviations ranged from a low of -.001 to as high as +0.064 for the twenty-five hydrous-silicates discussed.

Similarly, synthetic hydrous micas of this study display consistently positive deviations of $\bar{n}_{\text{calc.}}$ from $\bar{n}_{\text{obs.}}$. Only annites display a negative deviation, and positive deviations as high as +0.087 are noted. It would thus appear that the value cited for $k(H_2O)$ by Larsen and Berman (1934) of 0.034 cannot be applied directly to water in the silicate minerals. A significantly smaller value for $k(H_2O)$ is implied by the above data. Another source of error in the calculated K for silicates may result from erroneous k values for transition metals. Jaffee (1956) notes that $k(Fe_2O_3)$ varies from 0.290 in silicates to 0.404 in oxides. It thus appears that k for transition metals may be lowered considerably in a silicate environment. However, k values for copper, cobalt, nickel, etc. are known only for the oxide environment. This may, in part, explain the anomalously high values for \bar{n} calculated. It seems that further refinement of k values are needed before the rule of Gladstone and Dale may be effectively applied to silicate minerals.

TABLE 5. Optical Properties of Synthetic Hydrous Trioctahedral Micas

<u>Composition</u>	<u>α</u>	<u>γ</u>	<u>B</u>	<u>\bar{n}</u>	<u>\bar{n}</u>	<u>$\Delta\bar{n}$</u>	<u>Deviation</u>	<u>Color, Pleochroism & other remarks</u>	<u>Run# or Reference</u>
			<u>obs</u>	<u>obs</u>	<u>calc</u>				
<u>KMg₃AlSi₃O₁₀(OH)₂</u>	1.550 .002	1.587 .002	0.037	1.575	1.586	+0.011		Colorless, 2V=0°	
	1.550 .002	1.581 .001	0.031	1.571		+0.016	"	-	M#1
	1.548 .003	1.588 .003	0.040	1.575		+0.011	"	2V=0°	Wones (1966)
<u>Na⁺</u>	1.545 .003	1.569 .004	0.024	1.561	1.581	+0.020	Colorless		Yoder & Eugster (1954)
<u>Rb⁺</u>	1.540 .01	1.575 .01	0.035	1.560	1.647	+0.087	Colorless		Carman (1969) ⁴
<u>Cs⁺</u>	1.570 .01	1.605 .01	0.035	1.590	1.601	+0.011	Colorless		M#105
<u>Fe₃⁺²</u>	1.633 .002	1.700 .002	0.067	1.678	1.667	-0.011	Pleochroic: X = Red or yellow-brown Z = light green		Wones (1963b)
	1.636 .002	1.690 .002	0.055	1.672		-0.005			
<u>Co₃⁺²</u>	1.607 .002	1.668 .002	0.061	1.648	1.688	+0.040	Pale Purple to Lavendar		Wones & Carroll (1971) ⁵
<u>Ni₃⁺²</u>	1.614 .002	1.675 .002	0.061	1.654	1.702	+0.048	Medium green 2V=0°		M#114
	n.d.	1.652							M#115
<u>Cu₃⁺²</u>	1.588 .004	1.630 .004	0.042	1.616	1.690	+0.074	Medium blue		Klingsberg & Roy (1957)
<u>B⁺³</u>	1.549 .002	1.580 .002	0.031	1.570	1.581	+0.011	Colorless		M#29
	1.546 .002	1.568 .002	0.022	1.560		+0.021	"		M#108
<u>Ga⁺³</u>	1.558 .003	1.598 .003	0.040	1.585	n.d.	n.d.	Colorless		Eugster & Wright (1960)
	n.d.	1.598	-	-	-		-		M#109
<u>Fe⁺³</u>	1.601 .002	1.642 .002	0.041	1.628	1.656	+0.028	Pleochroic: X = reddish-brown Z = pale orange		Klingsberg & Roy (1957)
	1.600 .001	1.642 .001	0.040	1.629		+0.027	Colorless		M#111
<u>Ge₃⁺⁴</u>	1.596 .003	1.646 .003	0.050	1.623	n.d.	n.d.			Wise & Eugster (1964)
<u>Fe₃⁺²Fe₃⁺³</u>	1.705 .005	1.748 .003	0.043	1.734	1.711	-0.023	n.d.		M#63
<u>Co₃⁺²Fe₃⁺³</u>	1.715 .005	1.760 .005	0.0	1.745	1.787	+.042	x=red-brown z=pale purple		Wones (1963a)
<u>Ni₃⁺²Fe⁺³</u>	1.730 .005	1.770 .005	0.040	1.757	1.799	+.042	x=red-brown z=pale green		M#127
									M#123

1. $B = \gamma - \alpha$ 2. $\bar{n} = \sqrt{\alpha \gamma^2} \approx \frac{\alpha+2\gamma}{3}$ 3. $\bar{n}_{\text{calc.}} = \rho \cdot k + 1$, where ρ = density in gm/cm³ and k = specific refractive energy after the rule of Gladstone and Dale (1864).

4. Indices of refraction determined on mica heated to 80°C and immediately placed into oil.

5. Recent Mossbauer work reveals appreciable Fe⁺³ in all synthetic annites.

Sources of Error

The majority of trioctahedral micas synthesized represent 100% reaction from starting materials, and are thus assumed to be of ideal composition. However, rubidium and cesium phlogopites represented only \approx 20-25% of the reactants in those runs. These micas are thought to approximate ideal composition on the basis of the observed trioctahedral x-ray patterns and the predicted unit cell parameters. Due to difficulties in standardizing gallium in nitrate solution, the gallium phlogopite gel may be slightly deficient in Ga^{+3} , explaining why a maximum reaction of only 95% was obtained. Another possible source of error in the assumed compositions was revealed through Mössbauer studies of iron-bearing phlogopites. Roger Burns has shown a minimum of 10% Fe^{+3} in all annites, and from 5 to 15% Fe^{+2} in ferriphlogopites. Thus, one might also expect multiple valence states in Ni, Co and Cu-bearing micas. Seifert and Schreyer (1971) have demonstrated the presence of Mg^{+2} in tetrahedral coordination in Mg-rich synthetic trioctahedral micas. However, the assumption is made that all R^{+2} -cations in this study are in octahedral coordination unless noted otherwise.

In the investigation by Frondel and Ito (1966), and in this study, end-member zinc phlogopite $\text{KZn}_3\text{AlSi}_3\text{O}_{10}(\text{OH})_2$ was not achieved. In all experiments in which mica was produced, \geq 25% willemite- Zn_2SiO_4 with minor leucite and/or glass were also present. While the mica is clearly zinc-bearing, having cell parameters and indices of refraction

higher than phlogopite, the excess willemite is evidence of less than three Zn^{+2} atoms per mica formula unit. Neumann (1949) has well documented the great preference of zinc for tetrahedral coordination. Thus, one possible explanation for such a zinc-poor mica is that the zinc enters the tetrahedral layer, while aluminum fills the three octahedral sites; i.e., $KAl_3^{+3}(Zn_2^{+2}, Si_2^{+4})_3O_{10}(\text{OH})_2$. A structural study of the natural zinc mica hendricksite from Franklin, New Jersey, would aid in an understanding of zinc's role in the layer silicates.

Synthesis of end-member manganese phlogopite- $KMn_3AlSi_3O_{10}(\text{OH})_2$ was also unsuccessful. Frondel and Ito (1966) report that tephroite- Mn_2SiO_4 is present as a major phase in all mica-bearing runs, while in the present study pyrochroite- $Mn(\text{OH})_2$ accompanies the mica phase. Thus, while the unit cell parameters of the mica are greater than those of phlogopite, there are fewer than three manganese atoms per mica formula unit. Burns (1970, p. 43) has demonstrated from absorption spectra evidence that the distorted octahedral site of the phlogopite structure may stabilize manganese in the plus-three valence state. Furthermore, natural manganophyllites invariably contain aluminum in more than 10% of the octahedral sites. Therefore, the manganese-poor mica synthesized in this study may represent a solid solution between the components $KMn_3^{+2}AlSi_3O_{10}(\text{OH})_2 + KMn_2^{+3}AlSi_3O_{10}(\text{OH})_2 + KAl_2AlSi_3O_{10}(\text{OH})_2$. Further study on natural manganophyllites is needed to define the extent of Mn^{+3}/Mn^{+2} substitution

in the mica's distorted octahedral sites.

Relations between Cell Parameters and Ionic Radii

There exist several systematic relations between unit cell parameters and ionic radii of substituting cations. For example, the cell dimensions a_m , b_m and c_m are each proportional to the Shannon and Prewitt (revised 1970) ionic radii of cations substituting into the tetrahedral, octahedral or interlayer positions. This relation is clearly demonstrated by Figure One of b_m vs. octahedral cation ionic radii. The single exception to this rule is that of c_m vs. interlayer cation ionic radii (Fig. #2). The distinct negative curvature has been explained by Prewitt as the result of increasing coordination number of the interlayer cation with increasing ionic radii of this cation. For a given cation, an increase in coordination number is accompanied by a decrease in effective ionic radii. As expected, unit cell volumes are linearly related to the cube of the substituting cations' ionic radii for octahedral and tetrahedral substitutions, and display a slight negative curvature in the interlayer case (Figs. #3 and #4).

It is of interest to consider how b_m (the cell dimension within the mica layers) varies with respect to d_{001} (the dimension perpendicular to the layers) for each type of cation substitution. A plot of b_m vs. d_{001} (Fig. #5) demonstrates that octahedral, tetrahedral and interlayer cation substitutions have differing effects on the size and shape of the unit cell. For example, octahedral substitutions have a profound influence on b_m , while d_{001} remains virtually constant. The

near-vertical slope of the R^{+2} line is a result of this fact. On the other hand, interlayer cation substitutions alter the thickness d_{001} of the layers, while having a much smaller effect on b_m . R^{+3} and R^{+4} tetrahedral substitutions influence both b_m and d_{001} . It should be noted that these observations agree with the theoretical predictions of Takeda and Morimoto (1970).

Figure #1--Monoclinic b_m unit cell dimension vs. ionic radius of the octahedral cation for micas of the form $KR_3^{+2}AlSi_3O_{10}(OH)_2$. Black dots represent biotites on the join phlogopite--annite synthesized by Wones (1963b).

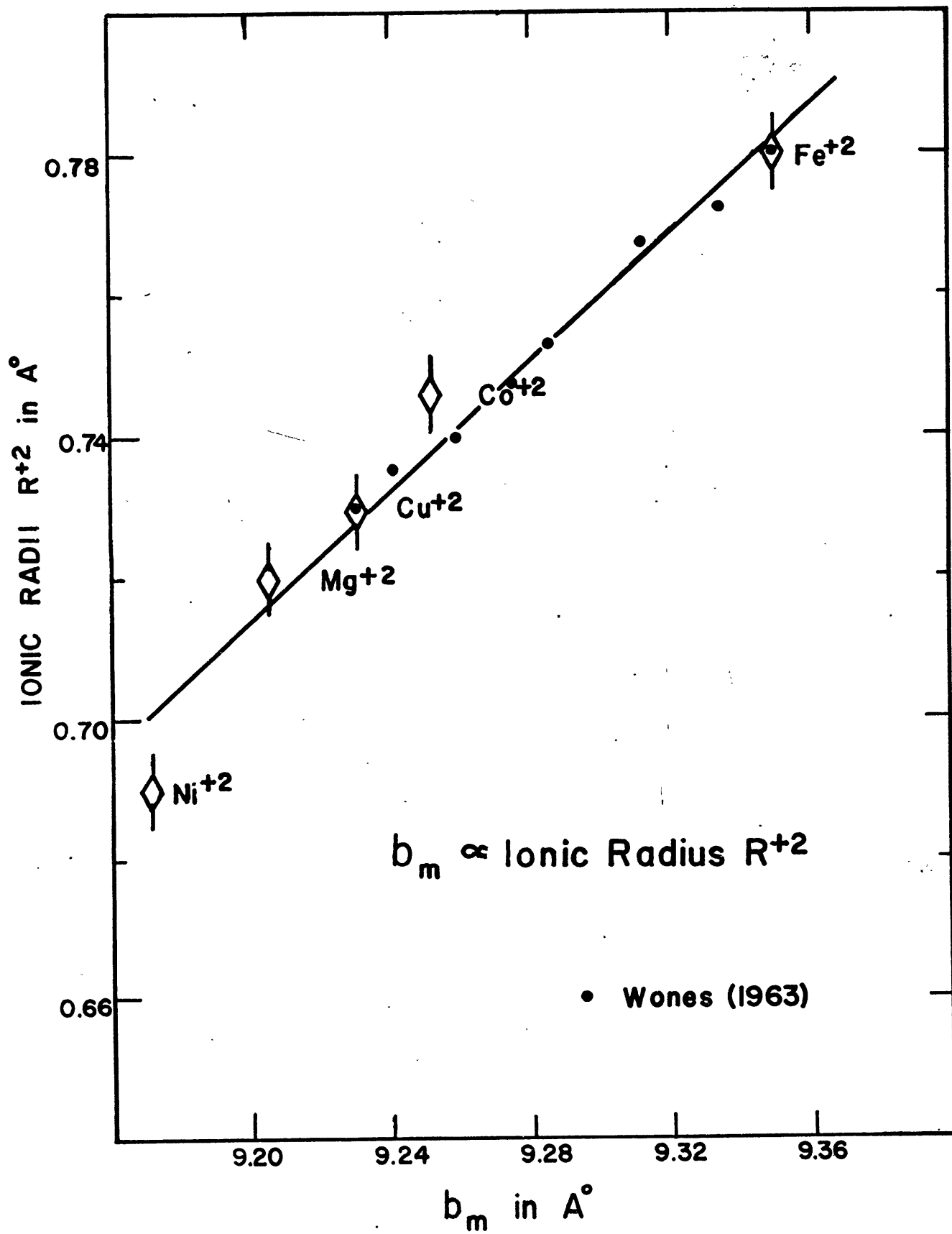


Figure #2--Monoclinic c_m unit cell dimension vs. ionic radius of the interlayer cation for micas of the form $R^+Mg_3AlSi_3O_{10}(OH)_2$.

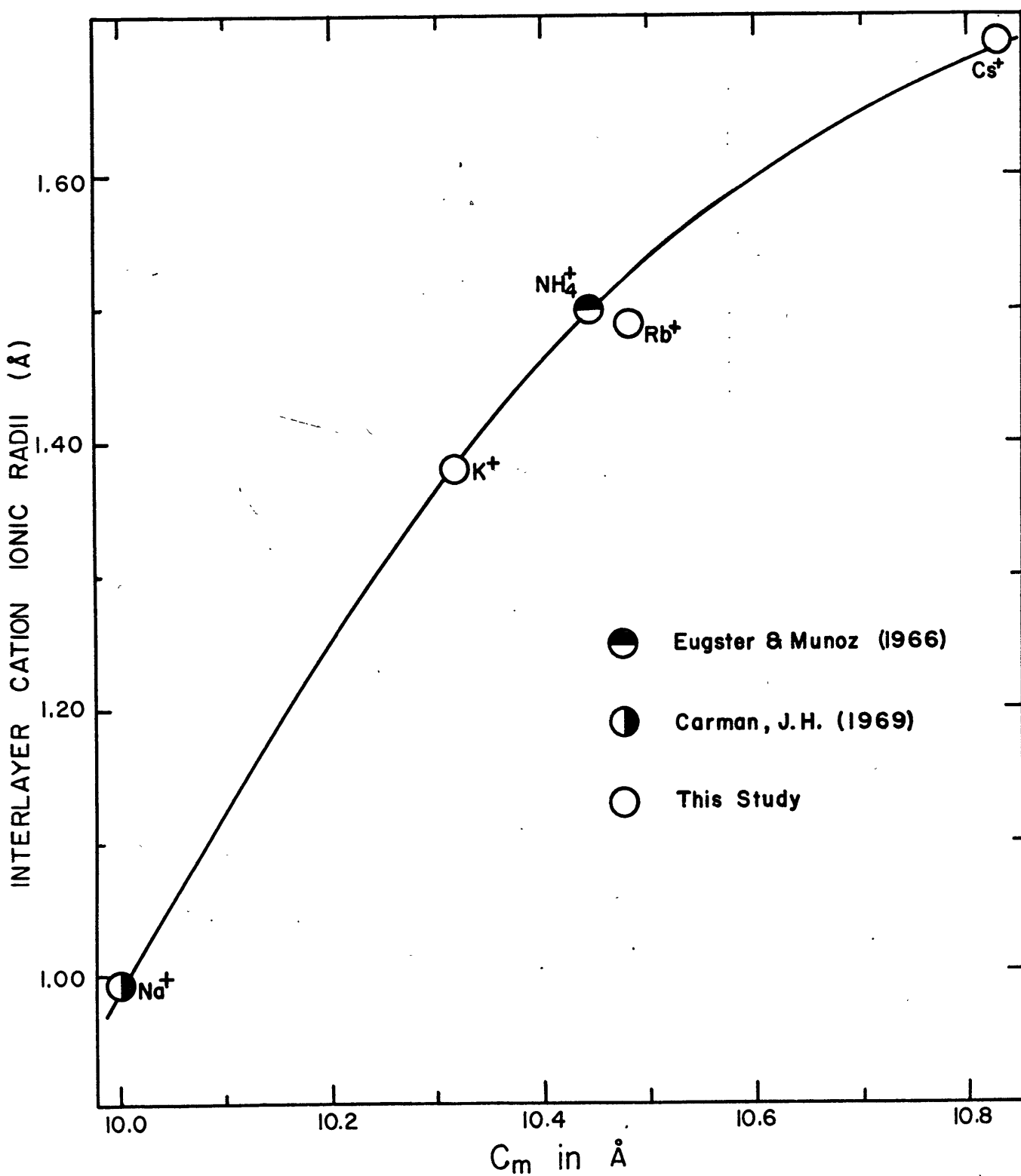


Figure #3--Monoclinic unit cell volume vs. ionic radius
of the octahedral R^{+2} cation cubed, for micas
of the form $KR_3^{+2}AlSi_3O_{10}(OH)_2$. Black dots
represent biotites on the join phlogopite--
annite synthesized by Wones (1963b).

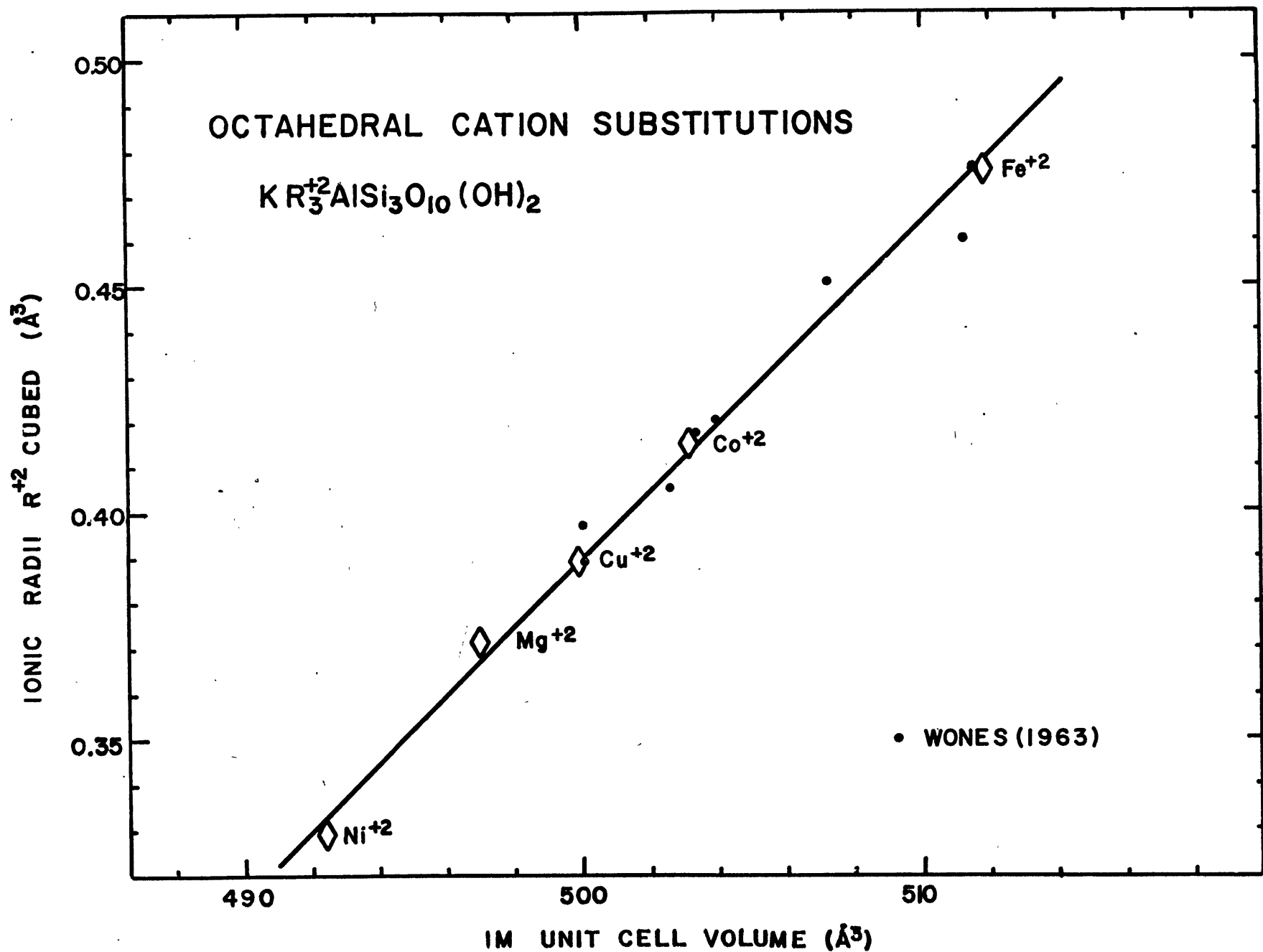


Figure #4--Monoclinic unit cell volume vs. the cube of
the interlayer R^+ cation radius for micas of
the form $R^+Mg_3AlSi_3O_{10}(OH)_2$, and vs. the cube
of the tetrahedral R^{+3} cation radius for micas
of the form $KMg_3R^{+3}Si_3O_{10}(OH)_2$.

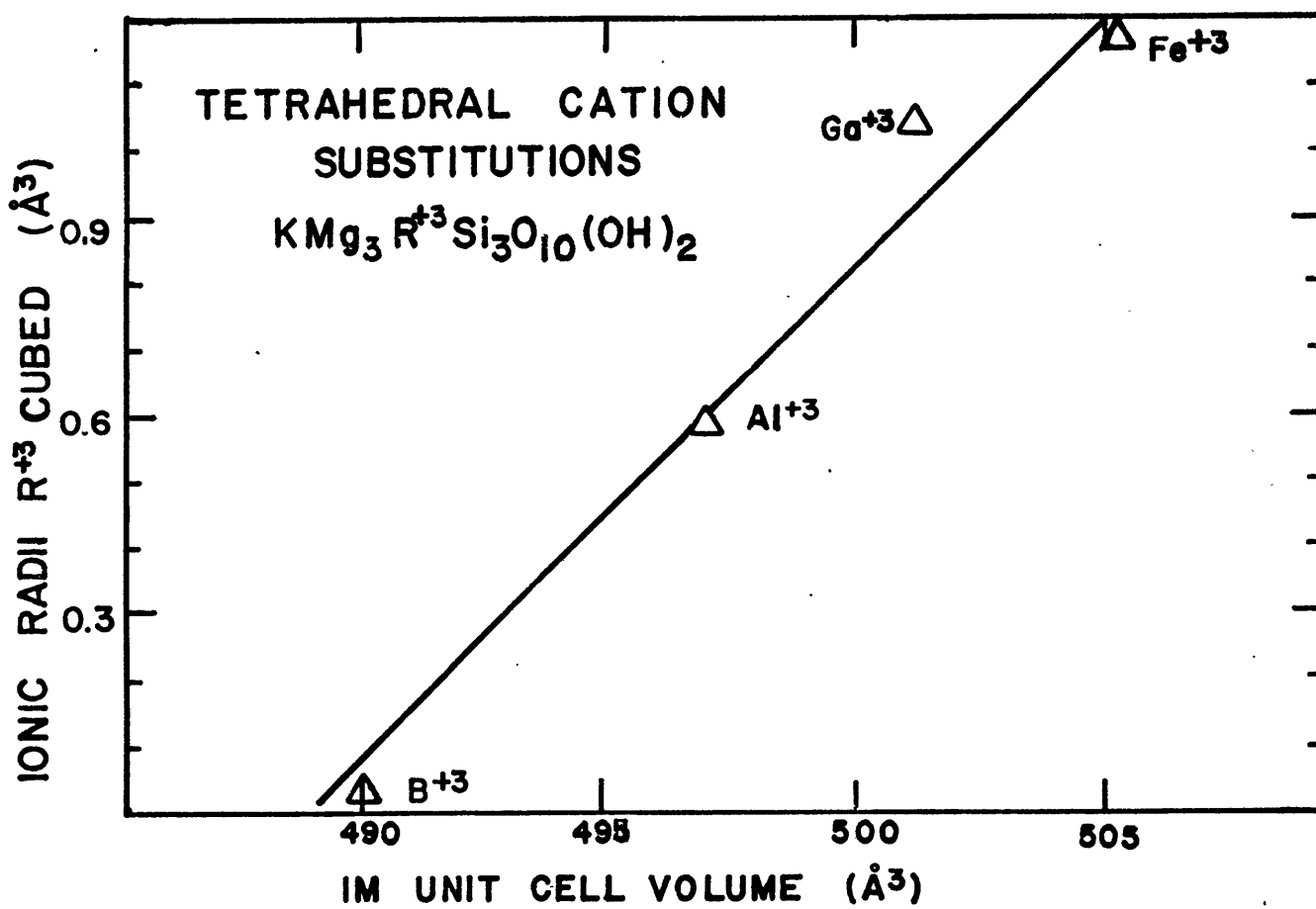
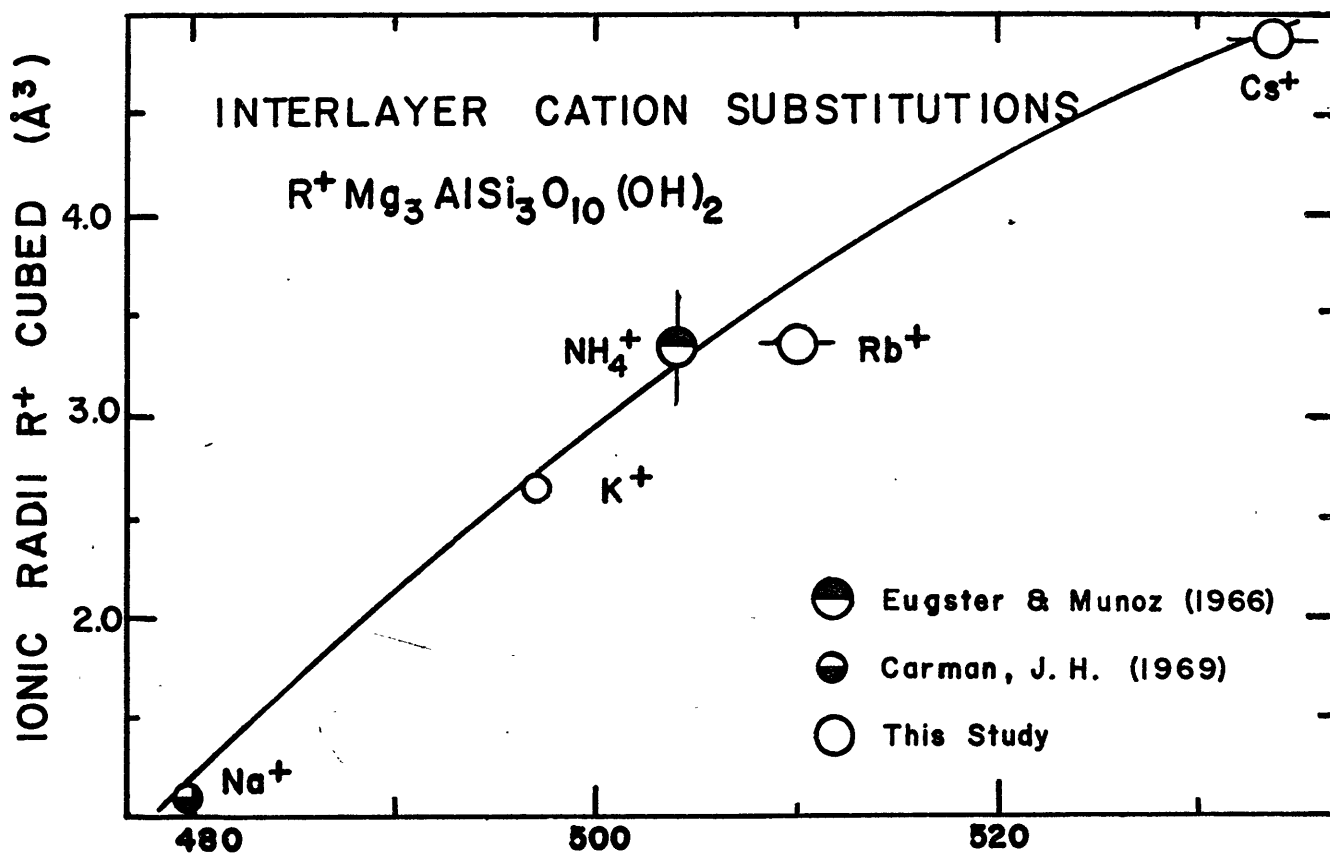
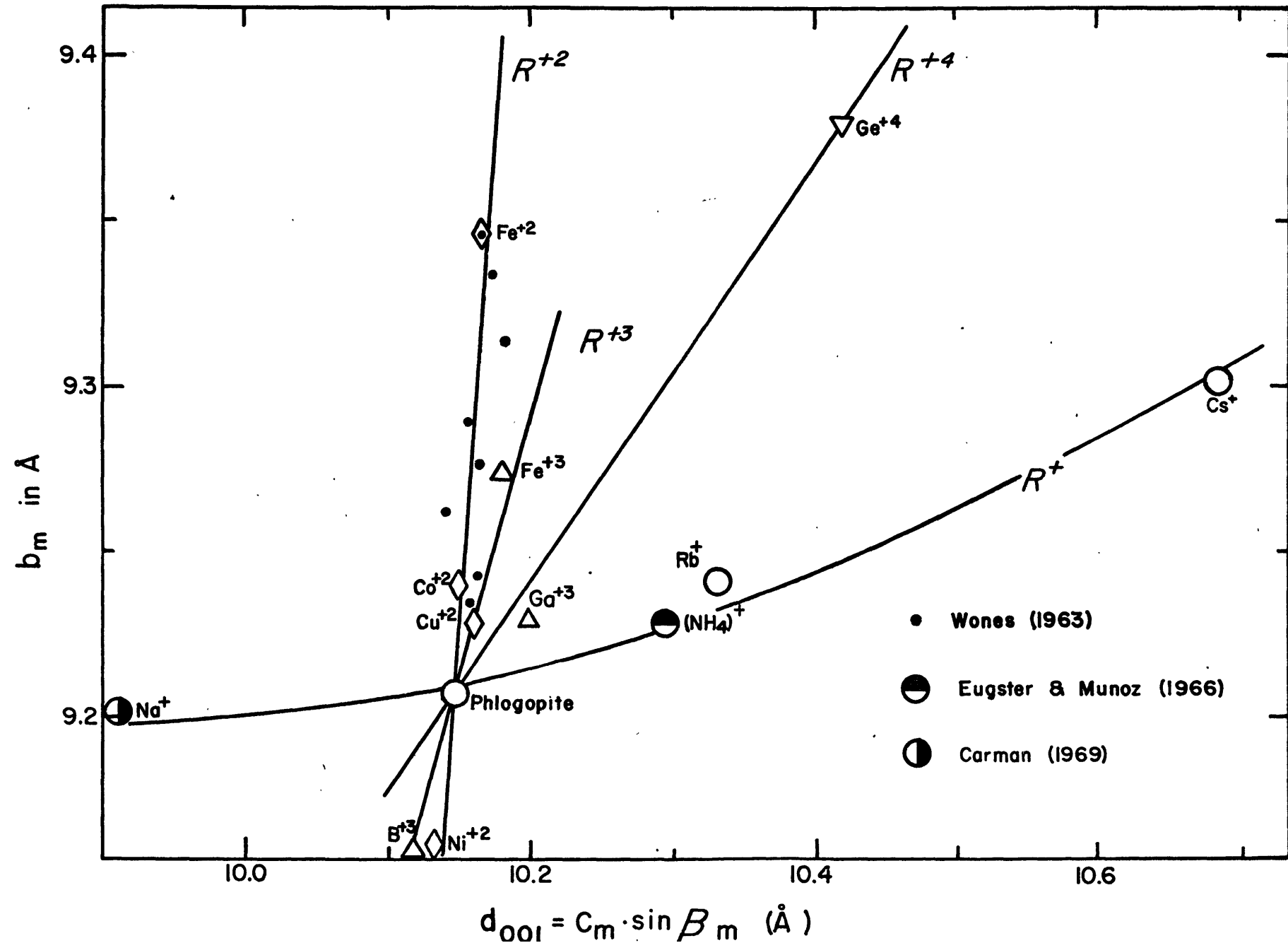


Figure #5--Monoclinic interlayer spacing d_{001} vs. monoclinic b_m cell dimension. The four lines represent micas of the form $KMg_3AlR_3^{+4}O_{10}(OH)_2$, $KMg_3R^{+3}Si_3O_{10}(OH)_2$, $KR_3^{+2}AlSi_3O_{10}(OH)_2$, and $R^+Mg_3AlSi_3O_{10}(OH)_2$.



Substitutions and Stability

Interlayer and tetrahedral cation substitutions demonstrate that a wide range of ionic radii are possible in these positions. Interlayer cations vary from sodium (ionic radius = 0.98 Å) to cesium (1.70). Tetrahedral cations from boron (0.12) to iron III (0.49) form stable micas. However, octahedral cations seem far more restricted in their ability to substitute into the phlogopite structure. No R^{+2} cation of radius greater than iron II (0.78), including lead (1.18) cadmium (0.95) and manganese (0.83), was found to form a stable mica. Furthermore, Eugster and Wones (1962) have demonstrated that the Fe^{+2} mica annite is far less stable than phlogopite. Thus, it appears that the stability of trioctahedral micas may be in part a function of the octahedral cation's ionic radius.

It is well known that in phlogopite the ideal $AlSi_3$ tetrahedral layer is larger than the Mg_3 layer (Radoslovich and Norrish, 1962). If the trioctahedral mica is to be stable, then these two layers must coincide, either by expansion of the octahedral layer along a_m and b_m or by contraction of the tetrahedral layer along a_m and b_m . Radoslovich and Norrish suggest four ways to accomplish this:

- 1) Altering bond lengths of the ideal layers,
- 2) tetrahedral layer tilting or corrugation,
- 3) octahedral layer flattening, or
- 4) tetrahedral layer rotation.

The altering of bond lengths is energetically far more difficult than altering bond angles. Thus, while such distortions have been noted in dioctahedral mica structure studies (Takeda and Burnham, 1969), bond stretching or contraction is assumed to be a minor effect. Tetrahedral tilting or corrugation is also well documented by Takeda and Burnham in their study of dioctahedral fluor-lithionite. However, these authors believe that tilting of tetrahedra will be minimized when all three octahedral positions are filled.

Donnay, Donnay and Takeda (1963) have demonstrated that the octahedral 001 projection may conform to the larger tetrahedral layer by octahedral layer flattening (See Fig. #6). In this way bond lengths are preserved while bond angles are altered. The amount of compression may be represented by the angle Ψ , which has the value $54^\circ 44'$ in an ideal octahedron. If the assumptions are made that:

- 1) there is no tetrahedral tilting or corrugation (i.e., basal oxygens in each tetrahedral sheet are coplanar),
- 2) 001 projections of tetrahedra are equilateral triangles, and
- 3) $a_m = b_m / \sqrt{3}$,

then Ψ is a simple function of the mean octahedral bond length d_o and cell dimension b_m : $\sin \Psi = b_m / 3\sqrt{3} \cdot d_o$. The mean octahedral bond length for $Mg-(O,OH)$ and $Fe^{+2}-(O,OH)$ are given by Donnay, Donnay and Takeda (1963) as 2.07 \AA° and 2.12 \AA° .

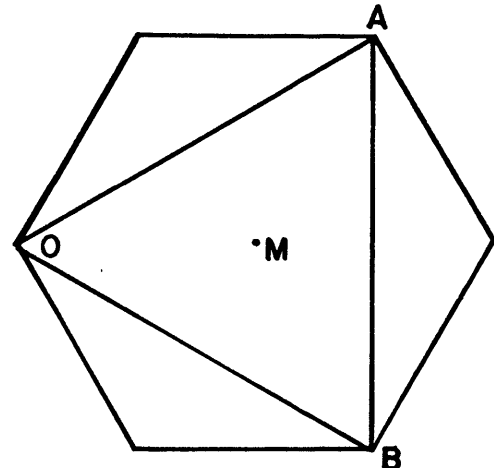
Figure #6--Expansion of the octahedral 001 projection by
octahedral layer compression.

OCTAHEDRAL LAYER COMPRESSION

$$\Psi = \text{Arc sin } (b_m / 3\sqrt{3} \cdot d_o)$$

$$b_m = 3 \cdot \overline{AB}$$

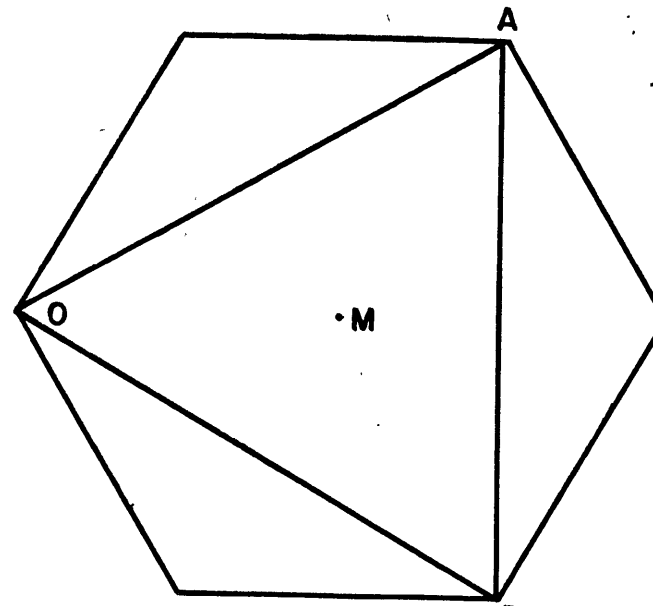
$$d_o = \overline{MO}$$



Ideal Octahedron:

$$\Psi = 54^\circ 44'$$

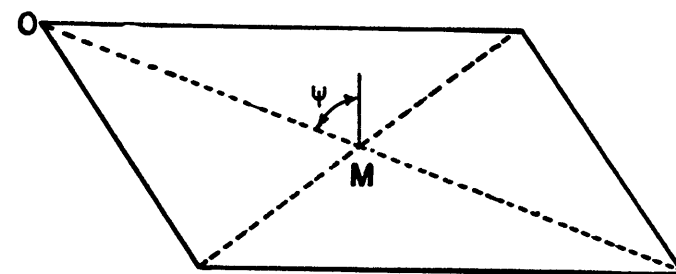
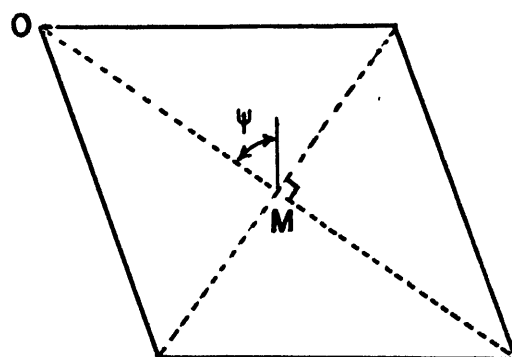
001
Projections



Flattened Octahedron:

$$\Psi > 54^\circ 44'$$

Y Axis
Projections



respectively. Mean bond lengths for other octahedral cations may be calculated by interpolation. Thus, knowing b_m , we can calculate Ψ for each octahedral layer substitution. In Figure #7, Ψ is plotted vs. octahedral cation ionic radius. As ionic radius increases, the value of Ψ is noted to decrease slightly. Thus, larger octahedral cations require less site flattening to expand the 001 octahedral projection. While octahedral layer flattening is a real effect in hydrous trioctahedral micas, this structural parameter does not explain the instability of 100% octahedral substitutions of cations larger than iron II.

Tetrahedral layer rotation is a fourth means of fitting the non-equivalent octahedral and tetrahedral layers (see Fig. #8). Donnay, Donnay and Takeda (1963) have shown that by rotating each tetrahedron through an angle α about an axis perpendicular to the 001 plane, the effective size of the tetrahedral sheet is reduced. Structure studies by Steinfink (1962) and others reveal values for α may be greater than 10° in natural micas. Thus, in phlogopite the strain between octahedral and tetrahedral layers may be released primarily through tetrahedral layer rotation.

If the conditions assumed by Donnay, Donnay and Takeda (1963) for octahedral layer flattening are correct, then α is defined by the mean tetrahedral bond length d_t and the cell dimension b_m : $\cos \alpha = b_m / 4\sqrt{2} \cdot d_t$. The mean tetrahedral bond length for the AlSi_3 layer is known to be $1.643 \pm .002 \text{ \AA}$ from studies of muscovite (Guven, 1967 and Burnham and

Figure #7--Octahedral layer compression angle Ψ vs. ionic radius of the octahedral R^{+2} cation in micas of the form $KR_3^{+2}AlSi_3O_{10}(OH)_2$. Black dots represent biotites on the join phlogopite--annite synthesized by Wones (1963b).

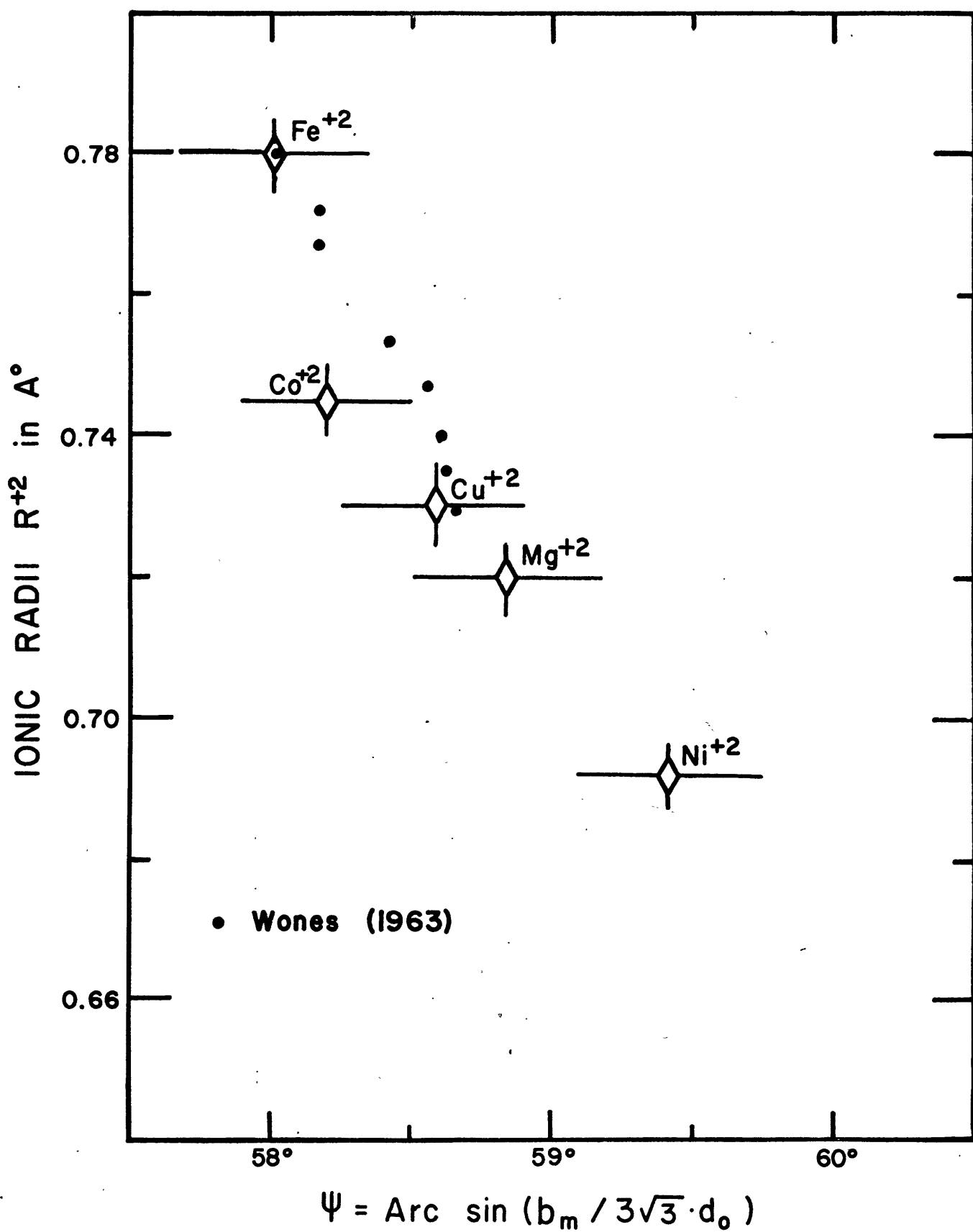
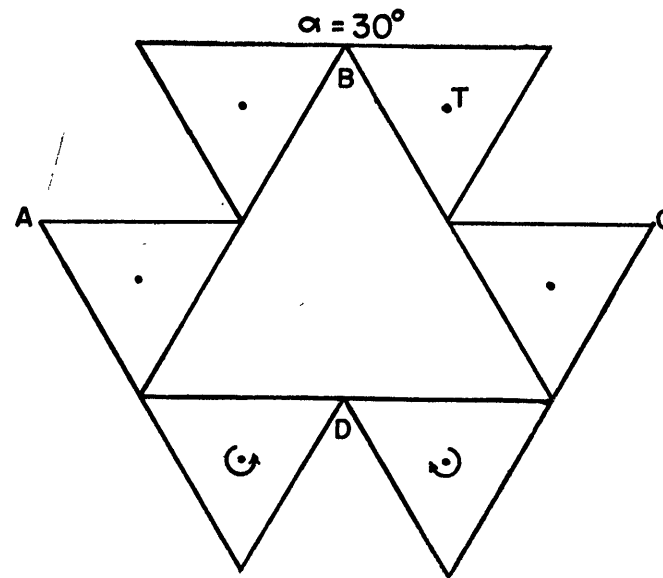
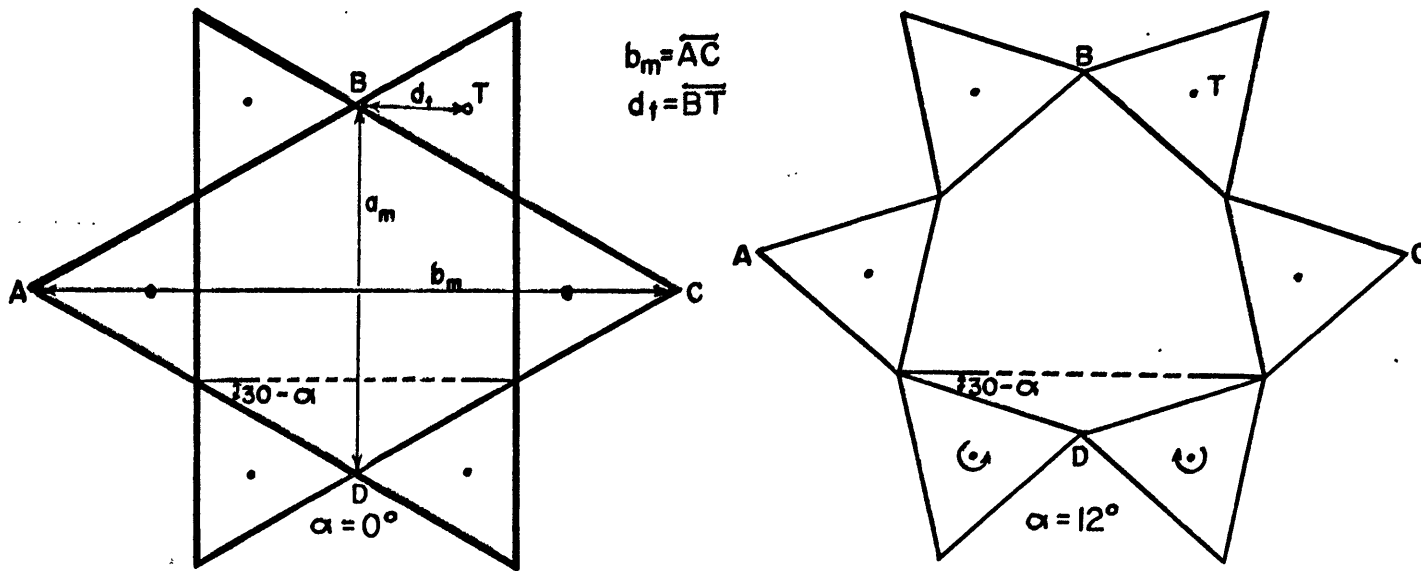


Figure #8--Contraction of the tetrahedral 001 projection
by tetrahedral layer rotation.

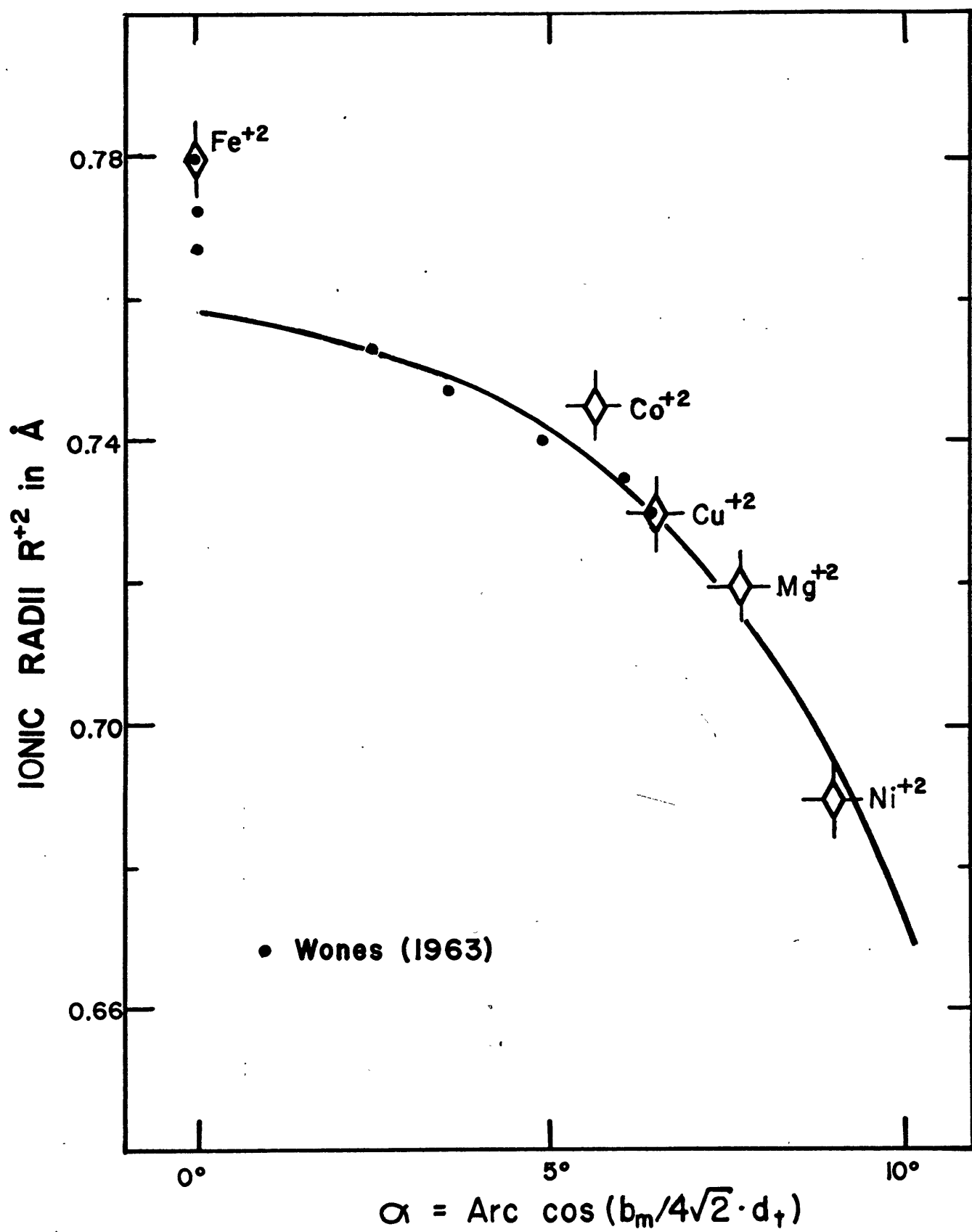
TETRAHEDRAL LAYER ROTATION α

$$\alpha = \text{Arc cos} (b_m / 4\sqrt{2} \cdot d_1)$$



Radoslovich, 1964), biotite (Franzini, 1963) and fluor-phlogopite (McCauley, 1968). With this value of d_t , and the known values of b_m , a plot of R^{+2} ionic radius vs. α has been constructed for micas of the form $KR_3^{+2}AlSi_3O_{10}(OH)_2$ (see Fig. #9). As the octahedral cation ionic radius increases to 0.76 \AA° , α approaches the critical value of 0° . For octahedral cations of ionic radius greater than $\approx 0.76 \text{ \AA}^\circ$, the tetrahedral layer cannot expand further by rotation. It might therefore be expected that hydrous trioctahedral micas with an $AlSi_3$ tetrahedral layer would not be stable for an octahedral layer cation of radius greater than about 0.76 \AA° .

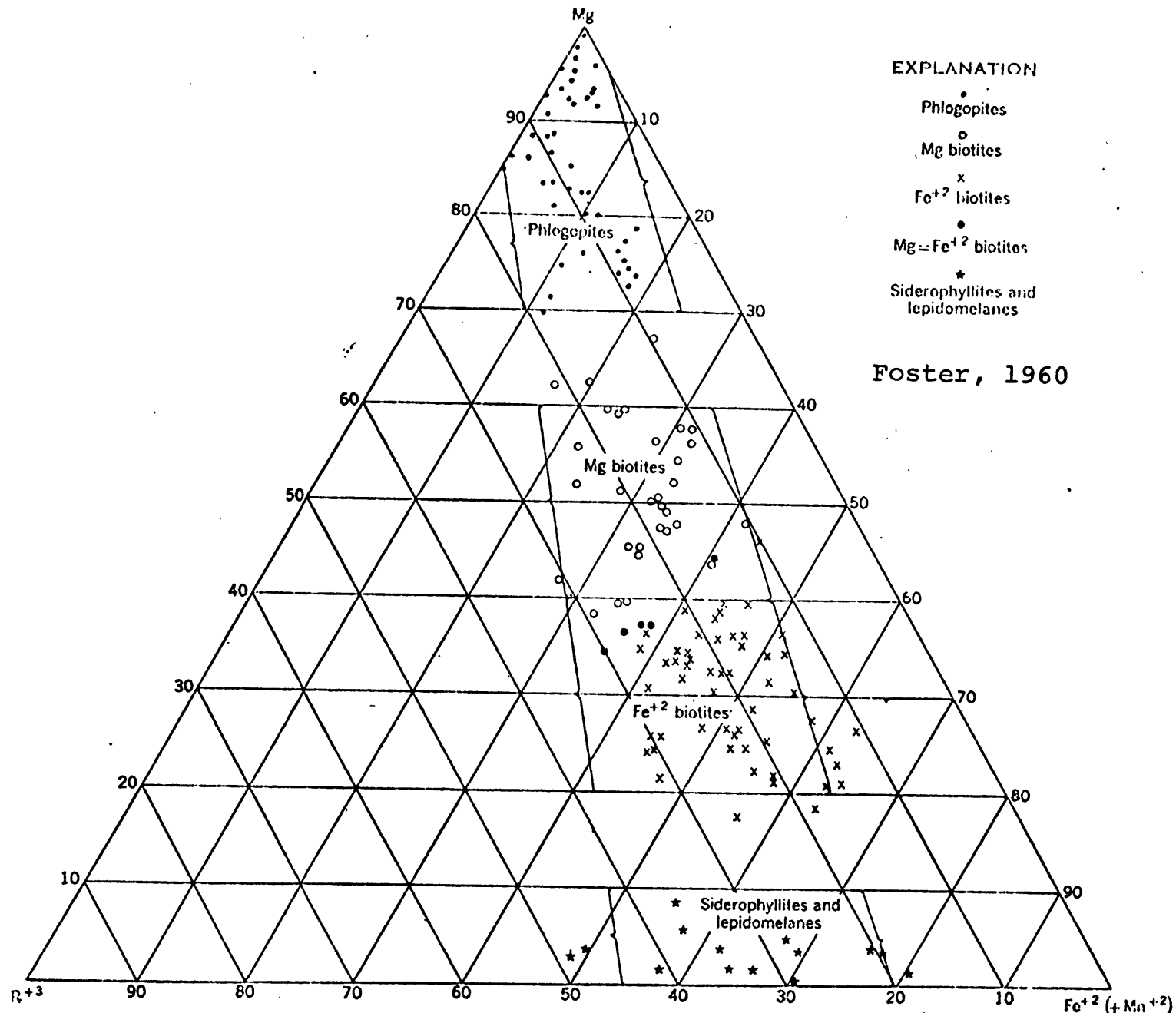
Figure #9--Tetrahedral layer rotation angle α vs. ionic radius of the octahedral R^{+2} cation for micas of the form $KR_3^{+2}AlSi_3O_{10}(OH)_2$. Black dots represent biotites on the join phlogopite--annite synthesized by Wones (1963b).



Octahedral Cation Distribution in Natural Micas

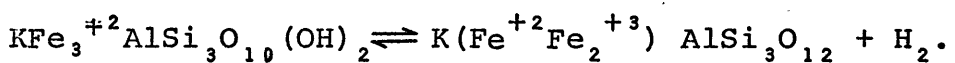
Foster (1960) has plotted the octahedral cation distribution for over 200 natural phlogopites, biotites and siderophyllites (Fig. #10). As the iron II content of these micas increases, so does the octahedral aluminum content. Trivalent aluminum in R^{+2} sites requires a corresponding substitution of aluminum for silicon in the tetrahedral layer. Thus, aluminum has the dual effect of increasing the size of the tetrahedral layer, while decreasing the effective octahedral cation radius. The maximum observed effective octahedral ionic radius, for the most iron-rich, aluminum-poor specimens, is 0.74 \AA° . Similarly, manganophyllites are known with almost 20% MnO substituting for MgO (Jakob, 1925), resulting in an effective octahedral ionic radius of 0.74 \AA° . Thus, while octahedral cations in natural micas of the form $KR_3^2\text{AlSi}_3\text{O}_{10}(\text{OH})_2$ approach the critical ionic radius of 0.76 \AA° , they are not observed to exceed this value.

Figure #10--The composition of the octahedral layer of
more than 200 natural phlogopites, biotites
and siderophyllites from Foster (1960).



The Composition of Annite

Synthetic annite was noted to be the only hydrous tri-octahedral mica of the form $KR_3^{+2}AlSi_3O_{10}(OH)_2$ which appears to have an average octahedral ionic radius greater than the critical value of 0.76 \AA° . Eugster and Wones (1962) have demonstrated that trivalent iron (VI ionic radius = 0.63 \AA°) may substitute for octahedral divalent iron (0.78 \AA°) in annite as expressed by the oxyannite reaction:



An annite with ≈ 12 mole percent octahedral Fe^{+3} (i.e. ≈ 18 mole percent oxyannite) has an average octahedral cation radius of 0.76 \AA° , and it was thus predicted that even the most reduced synthetic annites may have appreciable oxyannite content. Subsequent study by Wones, Burns and Carroll (1971) employing Mössbauer and analytical chemistry techniques have confirmed that at least 10 mole % of octahedral iron in all synthetic annites is in the trivalent state. It therefore appears that octahedral cation size restrictions, resulting from the misfit between octahedral and tetrahedral mica layers, may have a profound effect on the valency of iron in annite.

From Fig. #9 it can be seen that for synthetic biotites of high iron content, tetrahedral rotation (i.e., α) is zero. Therefore, from Donnay, Donnay and Takeda (1963):

$$\cos \alpha = 1 = b_m / 4 \cdot \sqrt{2} \cdot d_t \text{ for these micas.}$$

However, Wones (1963b) has shown that values for b_m increase

with increasing Fe content, in these high-iron biotites. It must therefore be assumed that d_t is also increasing in order to maintain the relation $b_m/d_t = 4\sqrt{2}$ for these micas. One possible way to increase the mean tetrahedral bond length d_t is by substitution of Fe^{+3} for Al^{+3} in the tetrahedral layer. Since b_m for annite = 9.348 \AA° , then $d_t = 9.348/4\sqrt{2} = 1.652 \text{ \AA}^\circ$. Donnay, Donnay and Takeda (1963) have suggested a value of 1.68 \AA° for d_t of the FeSi_3 tetrahedral layer, as opposed to the smaller 1.643 \AA° mean tetrahedral bond length for an AlSi_3 sheet. Therefore, $d_t = 1.652$ implies a composition of $(\text{Fe}_{0.2}^{+3}, \text{Al}_{0.8}^{+3}) \text{ Si}_3$ (i.e. $\approx 7\%$ total iron is trivalent and in tetrahedral sites) for annites' tetrahedral layer. Indeed, Mössbauer studies by Burns (see Wones, Burns and Carroll, 1971) confirm that 6.5% total Fe is tetrahedral Fe^{+3} !

Prediction of Trioctahedral Mica Stability

It has been shown that b_m is proportional to the octahedral cation ionic radius (Fig. #1). But we know that $\cos \alpha$ is proportional to b_m/d_t . Therefore, $\cos \alpha$ is proportional to octahedral ionic radius/ d_t . This linear relation is demonstrated in Figure #11, a plot of $\cos \alpha$ vs. R^{+2} ionic radii for varying mean tetrahedral bond length d_t . The line for an AlSi_3 tetrahedral layer ($d_t = 1.643$) has been developed previously (Fig. #9). Donnay, Donnay and Takeda (1963) suggest a value of $d_t = 1.68 \text{ \AA}$ for the FeSi_3 tetrahedral layer, and this value has been used to obtain a second line on Figure #11 defined by Ni^{+2} , Mg^{+2} , Co^{+2} and Fe^{+2} ferri-phlogopites. By noting that these two lines are parallel, and by calculating additional mean tetrahedral bond lengths from data of Shannon and Prewitt (rev. 1970), additional lines can be drawn for the BSi_3 , GaSi_3 , and AlGe_3 tetrahedral layers. The resulting nomogram is found in Figure #12. The intersection of any line with $\cos \alpha = 1.00$ defines the critical octahedral cation radius for a hydrous trioctahedral mica with a mean tetrahedral bond length corresponding to that line. Thus, if the composition of a hydrous trioctahedral mica is known, systematic relations between composition and ionic radii enable us to predict unit cell dimensions, structural parameters, and even the stability of the mica.

Figure #11--Cosine of the tetrahedral layer rotation angle α vs. octahedral cation radius for micas of the form $KR_3^{+2}(AlSi_3)O_{10}(OH)_2$ [$d_t = 1.643 \text{ \AA}^{\circ}$] and of the form $KR_3^{+2}(FeSi_3)-O_{10}(OH)_2$ [$d_t = 1.68 \text{ \AA}^{\circ}$].

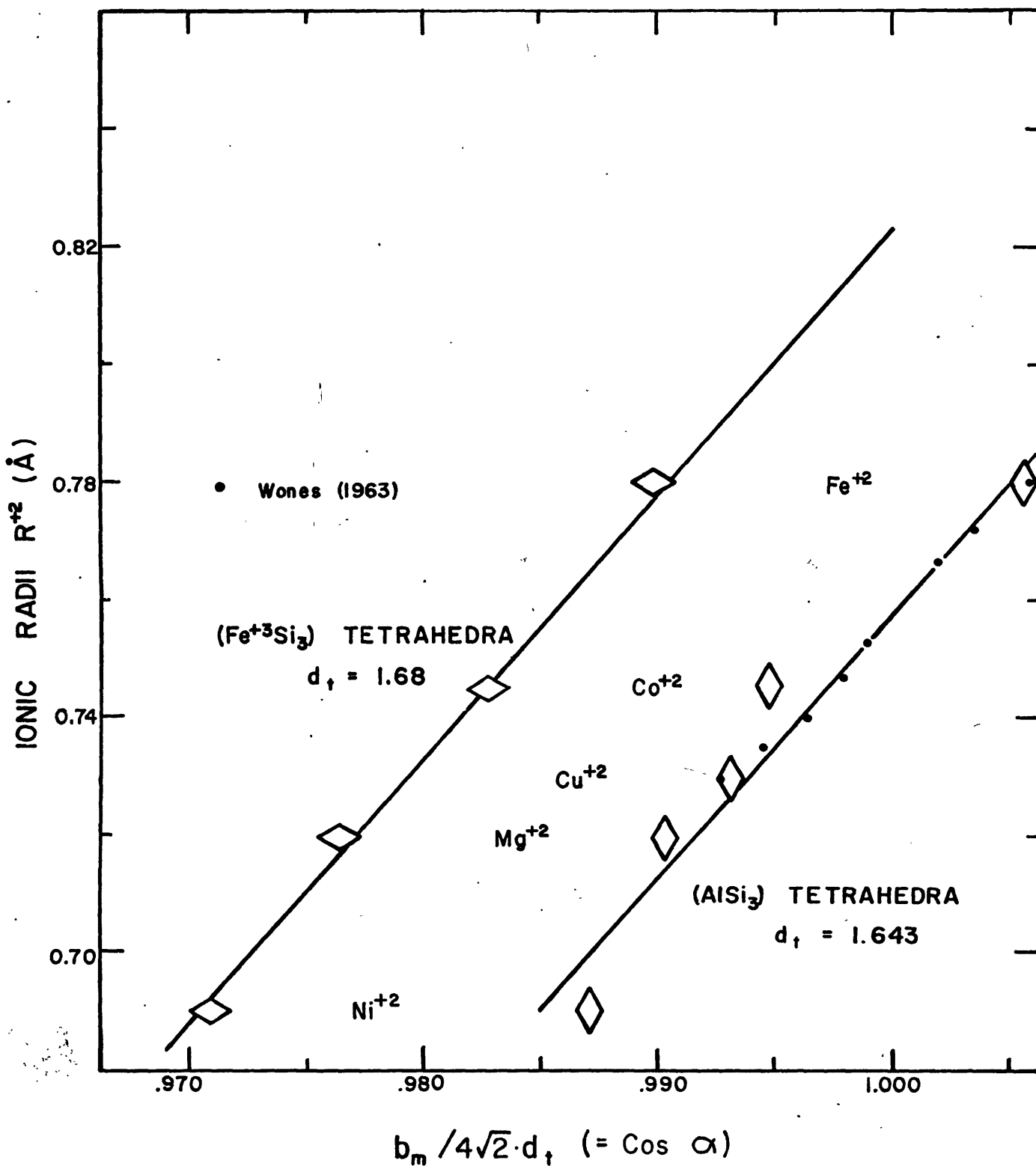
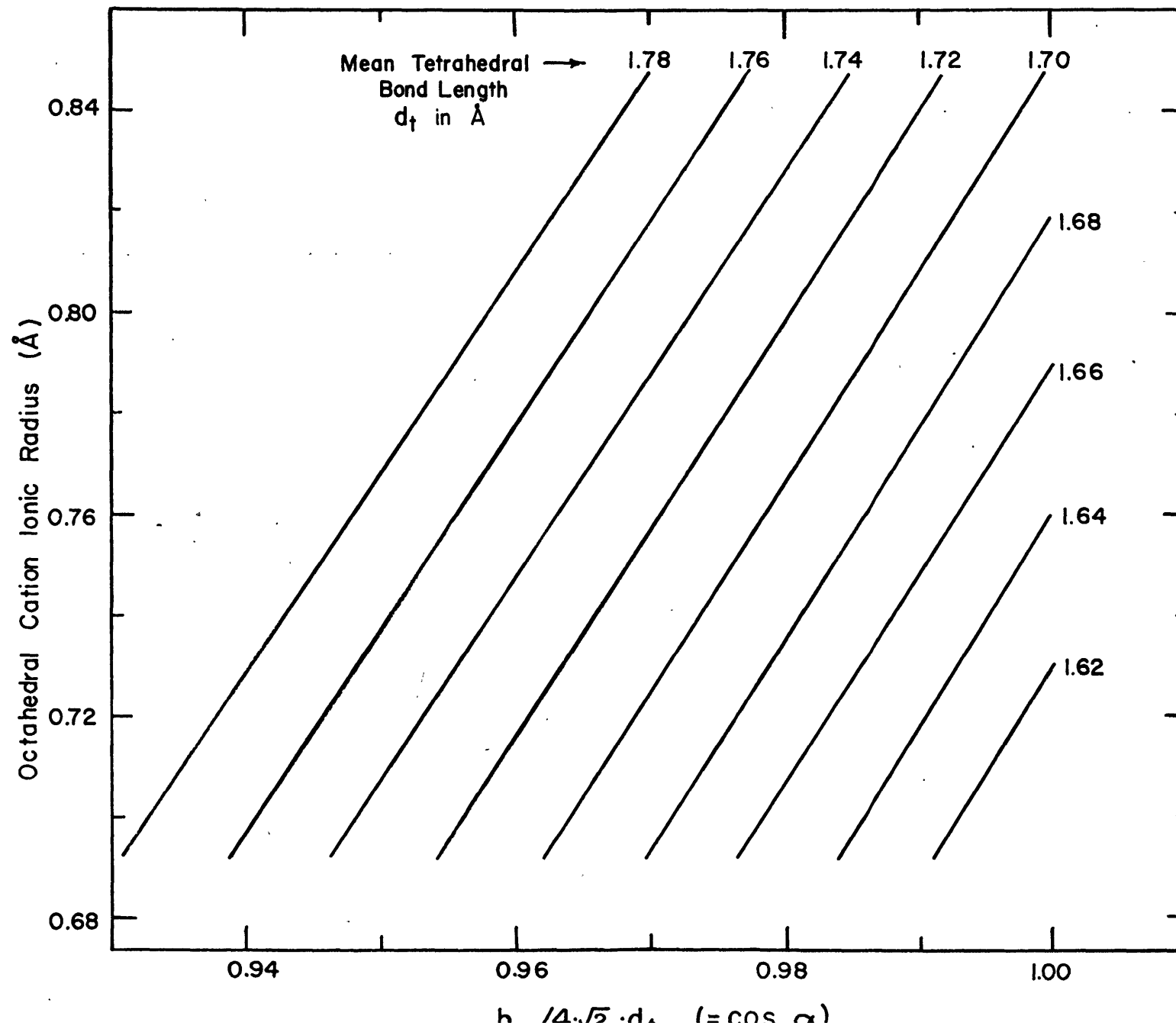


Figure #12--A nomogram for $\cos \alpha$ vs. octahedral R^{+2}
cation radius vs. mean tetrahedral bond
length d_t for all hydrous, potassic, tri-
octahedral micas.



FUTURE STUDIES

Several future studies are suggested by the present work. Of primary importance is the need for a structure determination of a hydrous trioctahedral mica. While nearly pure specimens of natural hydrous phlogopite exist (Foster, 1960), no x-ray crystal structural study of such a mica has been published. Structure studies of natural Zn and Mn micas would enhance our understanding of both mica structure and the role of Zn and Mn in these hydrous silicates.

It is well known that transition metal cations may induce site distortions in silicates. Examinations of the absorption spectra of Ni, Cu, Co, Fe and Mn-bearing micas might provide information regarding the nature and extent of such distortions.

The greatest difficulty in performing x-ray and spectral single crystal work on synthetic hydrous micas is that such crystallites rarely exceed 20μ in diameter. A technique for growing larger crystals under hydrothermal conditions would benefit both this and many other researches. Several alterations in the standard hydrothermal apparatus might facilitate single crystal growth. The use of higher ratios of H_2O to starting material might increase mobility of solids while decreasing the number of nucleation sites. A larger volume of starting materials, requiring a larger capsule, might also aid in macrocrystal development. A third technique for increasing crystallite size might be to super-

impose a directional stress onto the hydrothermal system. Such a directional stress field might lower the surface free energy of large crystals.

As mentioned previously, the refractive energies of water and transition metals in silicates are not well known. A systematic study of hydrous silicate indices of refraction vs. composition would enable more meaningful applications of the rule of Gladstone and Dale.

The present study by no means has considered all possible end-member micas. Rather, it demonstrates the vast number of synthetic micas, of both end-member and intermediate compositions, that may be produced with relative ease. Future studies on the effects of cation substitutions on the physical properties of dioctahedral micas and fluor-trioctahedral micas would enhance our present understanding of the sheet silicate structure. Indeed, the method of cation substitution in silicate minerals can provide useful information about virtually every silicate structure.

References

- Barnes, H.L. and W.G. Ernst (1963) Ideality and ionization in hydrothermal fluids: The system MgO-H₂O-NaOH. Amer. Jour. Sci., 261, 129-150.
- Burnham, C.W. and E.W. Radoslovich (1964) Crystal structures of coexisting muscovite and paragonite. Carnegie Inst. Wash. Yearb., 63, 232-236.
- Burns, R.G. (1970) Mineralogical Applications of Crystal Field Theory. Cambridge University Press, Cambridge, England, 224p.
- Carman, J.H. (1969) The study of the system NaAlSiO₄-Mg₂SiO₄-SiO₂-H₂O from 200 to 5000 bars and 800°C to 1100°C and its petrologic applications. Ph.D. Thesis, Penn. State Univ. 290p.
- Crowley, M.S. and R. Roy (1960) The effect of formation pressure on sheet structures - a possible case of Al-Si ordering. Geochim. Cosmochim. Acta, 18, 94-100.
- DeVries, R.C. and R. Roy (1958) The influence of ionic substitution on the stability of micas and chlorites. Econ. Geol., 53, 958-965.
- Donnay, G., J.D.H. Donnay and H. Takeda (1964) Trioctahedral one-layer micas. II. Prediction of the structure from composition and cell dimensions. Acta Cryst., 17, 1371-1381.
- Edison, T.A. (1916) U.S. Patent #1,167,484. Chem. Abstracts, 10, 725.
- Eugster, H.P. (1957) Heterogeneous reactions involving

- oxidation and reduction at high pressures and temperatures.
J. Chem. Phys., 26, 1160.
- Eugster, H.P. and J. Munoz (1966) Ammonium micas: Possible sources of atmospheric ammonia and nitrogen. Science, 151, 683-686.
- Eugster, H.P. and D.R. Wones (1962) Stability relations of the ferruginous biotite, annite. J. Petrol., 3, 82-125.
- Eugster, H.P. and T.L. Wright (1960) Synthetic hydrous boron micas. U.S. Geol. Survey PP400, B441-B442.
- Figlarz, M. and F. Vincent (1968) Sur la déshydration de l'hydroxyde de cobalt $\text{Co}(\text{OH})_2$. C.R. Acad. Sc. Paris, 266, 376-378.
- Foster, M.D. (1960) Interpretation of the composition of trioctahedral micas. U.S. Geol. Survey PP 354-B, 11-46.
- Franzini, M. (1963) On the crystal structure of biotite. Zeit. Krist., 119, 297-309.
- Franzini, M. (1969) The A and B mica layers. Contrib. Mineral. Petrol., 21, 203-224.
- Frondel, C. and J. Ito (1966) Hendricksite, a new species of mica. Amer. Mineral. 51, 1107-1123.
- Gladstone, J.H. and T.P. Dale (1864) Researches on the refraction, dispersion, and sensitiveness of liquids. Phil. Trans. Roy. Soc. London, 153, 337-348.
- Güven, N. (1967) The crystal structure of 2M_1 phengite and 2M_1 muscovite. Carnegie Inst. Wash Yearb. 66, 487-492.
- Hatch, R.A., R.A. Humphrey, W. Eitel and J.E. Comeforo (1957) Synthetic mica investigations. IX. Review of progress

- from 1947-1955. U.S. Bureau of Mines, Rept. Inv. 5337.
- Jaffe, H.W. (1956) Application of the rule of Gladstone and Dale to minerals. Amer. Mineral., 41, 757-777.
- Jakob, J. (1925) Beitrage zur chemischen konstitution der glimmer. I. Mitteilung: die schwedischen manganophylle. Zeit. Krist., 61, 155.
- Klingsberg, C. and R. Roy (1957) Synthesis, stability and polytypism of mickel and gallium phlogopite. Amer. Mineral., 42, 629-634.
- Larsen, E.S. and H. Berman (1934) The microscopic determination of the nonopaque minerals. U.S. Geol. Surv. Bull., 848, 266p.
- McCauley, J.W. (1968) Crystal structures of the micas $KMg_3 - AlSi_3O_{20}F_2$ and $BaLiMg_2AlSi_3O_{10}F_2$. Ph.D. Thesis, Penn. State Univ., 180p.
- Neumann, H. (1949) Notes on the mineralogy and geochemistry of zinc. Mineral. Mag., 28, 575-581.
- Pistorius, C.W.F.T. (1962) Thermal decomposition of the hydroxides of cobalt and nickel to 100 kilobars. Zeit. fur P. Chem., 34, 287-294.
- Prewitt, C.T. (1971) Private Communication.
- Radoslovich, E.W. (1960) The structure of muscovite, $KAl_2 - (Si,Al)O_{10}(OH)_2$. Acta Cryst., 13, 919-932.
- Radoslovich, E.W. (1962) The cell dimensions and symmetray of layer lattice silicates. II. Regression relations. Amer. Mineral., 47, 617-636.
- Radoslovich, E.W. and K. Norrish (1962) The cell dimensions

- and symmetry of layer lattice silicates. I. Some structural considerations. Amer. Mineral., 47, 599-616.
- Schairer, J.F. and N.L. Bowen (1955) The system $K_2O-Al_2O_3-SiO_2$. Amer. Jour. Sci., 253, 681-746.
- Seifert, F. and W. Schreyer (1971) Synthesis and stability of micas in the system $K_2O-MgO-SiO_2-H_2O$ and the relations to phlogopite. Contrib. Mineral. Petrol., 30, 196-215.
- Shannon, R.D. and C.T. Prewitt (1970) Revised values of effective ionic radii. Acta Cryst., 26, 1046-1048.
- Shaw, H. (1963) The four-phase curve sanidine-quartz-liquid-gas between 500 and 4000 bars. Amer. Mineral., 48, 883-896.
- Smith, J.V. [ed.] (1967) X-ray Powder Data File. American Society for Testing and Materials, Philadelphia, Pa.
- Smith, J.V. and H.S. Yoder (1956) Experimental and theoretical studies of the mica polymorphs. Mineral. Mag., 31, 209-235.
- Steinfink, H. (1962) Crystal structure of a trioctahedral mica: phlogopite. Amer. Mineral., 47, 886-896.
- Stubicon, V. and R. Roy (1962) Boron substitution in synthetic micas and clays. Amer. Mineral. 47, 1166-1173.
- Takeda, H. and C.W. Burnham (1969) Fluor-polylithionite: A lithium mica with nearly hexagonal $(Si_2O_5)^2$ ring. Mineral. Jour., 6, 102-109.
- Takeda, H. and N. Morimoto (1970) Crystal chemistry of rock-forming minerals. I. Structural studies of micas. Jour. Cryst. Soc. Japan, 112, 231-248.

- Tuttle, O.F. (1949) Two pressure vessels for silicate-water studies. Geol. Soc. Amer. Bull., 60, 1727-1729.
- Van My, M. le (1964) Étude microcalorimetrique des hydrates de cuivre et de nickel. Bull. Soc. Chem. France, 3, 545-549.
- Wise, W.S. and H.P. Eugster (1964) Celadonite: Synthesis, thermal stability and occurrence. Amer. Mineral., 49, 1031-1083.
- Wones, D.R. (1963a) Phase equilibria of "ferriannite," $KFe_3^{+2}Fe^{+3}Si_3O_{10}(OH)_2$. Amer. Jour. Sci., 261, 581-596.
- Wones, D.R. (1963b) Physical properties of synthetic biotites on the join phlogopite-annite. Amer. Mineral., 48, 1300-1321.
- Wones, D.R. (1967) A low pressure investigation of the stability of phlogopite. Geochim. Cosmochim. Acta, 31, 2248-2253.
- Wones, D.R., R. Burns, and B. Carroll (1971) Stability and properties of annite.(abs.) Trans. A.G. U., 52, 369-370.
- Wones, D.R. and H.P. Eugster (1965) Stability of biotite: Experiment, theory and application. Amer. Mineral., 50, 1228-1272.
- Yoder, H.S. and H.P. Eugster (1954) Phlogopite synthesis and stability range. Geochim. Cosmochim. Acta, 6, 157-185.

APPENDIX A--The stability of hydrous trioctahedral micas and their related hydroxides.

Introduction

It has been demonstrated that mica stability is closely related to the ionic radius of the octahedral cation. Radoslovich (1963) and others have noted that the octahedral layer of trioctahedral micas possesses a structure analogous to that of brucite-- $Mg(OH)_2$. Therefore, in conjunction with studies on the physical properties of hydrous trioctahedral micas, stability relations of nickel and cobalt micas and hydroxides are now being determined. While this work is not finalized, a preliminary report follows.

Several studies on the stabilities of hydrous trioctahedral micas and their related hydroxides have been presented by previous investigators. Brucite-- $Mg(OH)_2$ stabilities have been examined by several authors, the most frequently cited being that of Barnes and Ernst (1963). The hydroxide stabilities of cobalt and nickel have been determined by Pistorius (1962) for pressures from 5 to 100 kilobars. Van My (1964) and Figlarz and Vincent (1968) provide additional data on these stabilities. As mentioned previously (see Table One), several authors have examined stabilities of hydrous trioctahedral micas of the form $KR_3^{+2}AlSi_3O_{10}(OH)_2$. The most important of these studies are, for Mg^{+2} , Yoder and Eugster (1954) and Wones (1967); for Fe^{+2} , Eugster and Wones (1962) and Wones, Burns & Carroll

(1971); and for Ni^{+2} , Klingsberg and Roy (1957).

Experiments and Data

All stability experiments were performed in standard hydrothermal pressure apparatus as previously described. A partial list of synthesis experiments and resulting stability points thus far completed may be found in Table A-1. Slow quenching of pure CoO , Co(OH)_2 , NiO and Ni(OH)_2 from stability curve temperatures and pressures revealed no development of other phases. It is therefore assumed that no anomalous phase development took place in fast-quenching of these stability determination experiments.

In order to determine thermodynamic properties of the hydroxides and oxides of cobalt and nickel, the unit cell volumes of these substances have been redetermined (see Table A-2). While volume and cell parameters of CoO , Co(OH)_2 and NiO are in close agreement with those reported in the ASTM File (Smith (ed.), 1967), those of Ni(OH)_2 are somewhat lower than ASTM values. Future work will consider this discrepancy more carefully, and determinations of the cell parameters of Ni(OH)_2 formed at a range of temperatures will be performed.

Preliminary Conclusions

Data of Pistorius (1962) and of this study agree that Co(OH)_2 and Ni(OH)_2 dehydrate at much lower temperatures than Mg(OH)_2 , but are certainly more stable than Fe(OH)_2 .

TABLE A-1--Stability Experiments

a. Cobalt Hydroxide Dehydration: $\text{Co(OH)}_2 \rightleftharpoons \text{CoO} + \text{H}_2\text{O}$.

Pressure (bars)	Temperature (°C)	Duration (hrs.)	Reactants	Products
200	208	36	CoO	$\text{CoO} + \text{Co(OH)}_2$
200	214	36	Co(OH)_2	CoO
2000	240	32	CoO	$\text{CoO} + \text{Co(OH)}_2$
2000	244	48	Co(OH)_2	CoO

Stability Points: (200 \pm 2 bars, 211 \pm 3 °C)
 (2000 \pm 20 brs, 242 \pm 2 °C)*
 (5 \pm 1 kbars, 258 \pm 10 °C)*
 (15 \pm 1 kbars, 297 \pm 5 °C)*
 (27 \pm 1.5 kbs, 308 \pm 10 °C)*
 (50 \pm 2.5 kbs, 315 \pm 5 °C)*

b. Nickel Hydroxide Dehydration: $\text{Ni(OH)}_2 \rightleftharpoons \text{NiO} + \text{H}_2\text{O}$.

Pressure (bars)	Temperature (°C)	Duration (hrs.)	Reactants	Products
200	265	48	NiO	$\text{NiO} + \text{Ni(OH)}_2$
200	270	54	Ni(OH)_2	NiO
2000	275	38	NiO	Ni(OH)_2
2000	280	48	Ni(OH)_2	$\text{NiO} + \text{Ni(OH)}_2$
2000	285	48	Ni(OH)_2	NiO

Stability Points: (200 \pm 2 bars, 268 \pm 3 °C)
 (2000 \pm 20 brs, 280 \pm 5 °C)
 (5 \pm 1 kbars, 295 \pm 5 °C)*
 (16 \pm 1 kbars, 325 \pm 10 °C)*
 (31.5 \pm 1.5 kb, 330 \pm 15 °C)*
 (50 \pm 2.5 kb, 338 \pm 12 °C)*
 (100 \pm 5 kb, 345 \pm 5 °C)*

*--Data of Pistorius (1962)

Table A-1--Continued

c. Cobalt Mica Dehydration; $KCo_3AlSi_3O_{10}(OH)_2 \xrightarrow{\text{heat}}$
 $CoO + Co_2SiO_4 + KAlSi_2O_6$

Pressure (bars)	Temperature (°C)	Duration (hrs.)	Reactants	Products
100	790	48	Gel	Co Mica
100	795	48	Gel	Co Mica, CoO, Co_2SiO_4 & Leucite
100	802	32	Co Mica	CoO, Co_2SiO_4 , & Leucite
205	825	46	Gel	Co Mica
205	880	39	Gel	CoO, Co_2SiO_4 , & Leucite
300	875	48	Gel	CoO, Co_2SiO_4 , & Leucite

Stability Points: (100 \pm 1 bars, 796 \pm 6 °C)
(205 \pm 2 bars, 850 \pm 20 °C)

Table A-2--Cell Parameters and
hkl d-spacings for the Oxides and Hydroxides
of Cobalt and Nickel

a. Oxides:

<u>hkl</u>	<u>CoO</u>		<u>NiO</u>	
	<u>This Study</u>	<u>ASTM File</u>	<u>This Study</u>	<u>ASTM File</u>
111	2.4599	2.460	2.4108	2.410
200	2.1295	2.130	2.0881	2.088
220	1.5059	1.5062	1.4766	1.476
311	1.2840	1.2846	1.2596	1.259
222	1.2298	1.2298	1.2059	1.206
a (A°)	4.2595	4.260	4.17665	4.1769
Vol. (A°)³	77.281	77.31	72.859	72.872

b. Hydroxides:

<u>hkl</u>	<u>Co(OH)₂</u>		<u>Ni(OH)₂</u>	
	<u>This Study</u>	<u>ASTM File</u>	<u>This Study</u>	<u>ASTM File</u>
001	4.654	4.66	4.638	4.605
100	2.755	2.76	2.706	2.707
101	2.368	2.38	2.336	2.334
102	1.776	1.78	1.758	1.754
110	1.594	1.60	1.563	1.563
111	1.506	1.51	1.481	1.480
103	1.352	1.36	---	---
a (A°)	3.182	3.179	3.125	3.126
c (A°)	4.653	4.649	4.628	4.608
Vol. (A°)³	40.795	40.688	39.15	38.97

Brucite--Mg(OH)₂: a = 3.147 Å
 b = 4.769 Å
 Vol = 40.9026 Å³

which is metastable at laboratory conditions. Furthermore, Co(OH)_2 has a slightly lower thermal stability than Ni(OH)_2 . This relative sequence of stabilities: $\text{Fe(OH)}_2 < \text{Co(OH)}_2 < \text{Ni(OH)}_2 < \text{Mg(OH)}_2$, is identical to the order of stabilities seen in Fe^{+2} , Co^{+2} , Ni^{+2} and Mg^{+2} micas. Therefore, we may conclude that the factors which control the qualitative (if not quantitative) aspects of hydroxide stabilities may also strongly influence trioctahedral mica stabilities.

Ionic radii, crystal field stabilization, and oxidation potential of the octahedral cation are all known to affect the pressure-temperature stability of micas. Furthermore, octahedral cations affect the dehydration products of micas. While nickel and cobalt phlogopite react to form monoxide plus olivine plus leucite, Mg-phlogopite reacts to form kalsilite plus olivine plus leucite, and annite dehydrates to sanidine and magnetite! Clearly, the differences in ΔV_{rxn} for the decomposition of these four micas will affect the pressure stabilities. Accurate determinations of a variety of mica dehydrations will aid in our understanding of these controls on the stability of micas.

APPENDIX B--Selected computer d-spacing
output for synthetic micas.

On the following pages are computer output d-spacings
for the micas listed below:

<u>Formulae</u>	<u>Run Number</u>
KMg ₃ AlSi ₃ O ₁₀ (OH) ₂	M1
Ni ₃	M7b
Cu ₃	M49
Co ₃	M114
Zn ₃	M101
Mn ₃	M91
KMg ₃ B Si ₃ O ₁₀ (OH) ₂	M108
Ga	M109
Fe ⁺³	M111
KMg ₃ AlGe ₃ O ₁₀ (OH) ₂	M68

PHASES OF MONOCLINIC INDEXING.

FILE LISTING - *** PETERS II LIST

H	K	L	D CALC	D OBS	LAMBDA	2-THETA CALC	2-THETA OBS	2-THETA DIFF	
1	0	0	1	10.157771	1.540500	8.69766			
2	0	0	2	5.078984	1.540500	17.44595			
***	0	0	2	5.076884	5.077721	1.540500	17.44605	-0.00400	
3	0	2	0	4.602023	1.540500	16.27611			
***	0	2	0	4.602023	4.593786	1.540500	16.27011	-0.03487	
4	1	1	0	4.551393	1.540500	16.48656			
5	-1	1	1	4.406263	1.540500	20.13426			
6	0	2	1	4.151879	1.540500	21.17632			
7	1	1	1	3.939787	1.540500	22.54846			
***	1	1	1	3.939787	3.940392	1.540500	22.54846	0.00350	
***	1	1	-2	3.67347	3.670756	1.540500	24.20992	-0.01907	
8	-1	1	2	3.67347	1.540500	24.20992			
9	0	2	2	3.410279	1.540500	26.10704			
10	0	0	3	3.385922	1.540500	26.29820			
***	0	0	3	3.385922	3.388861	1.540500	26.29820	0.002321	
11	1	1	2	3.162913	1.540500	29.18941			
12	-1	1	3	2.934566	1.540500	30.43391			
***	1	1	-3	2.934566	2.935878	1.540500	30.43391	0.01393	
13	0	2	3	2.727283	1.540500	32.80481			
***	0	2	3	2.727283	2.727270	1.540500	32.81000	-0.00019	
14	-2	0	1	2.647665	1.540500	33.62565			
15	1	3	0 R	2.647127	2.643923	1.540500	33.83276	-0.04224	
16	2	0	0	2.618215	1.540500	34.21783			
17	-1	3	1 R	2.617649	2.617693	1.540500	34.22543	0.00046	
18	1	1	3	2.541001	1.540500	35.29120			
19	0	0	4	2.539441	1.540500	35.31360			
***	0	0	4	2.539441	2.539445	1.540500	35.31360	-0.00137	
20	-2	0	2	2.509372	1.540500	35.71095			
21	1	3	1 R	2.509956	2.508080	1.540500	35.75701	-0.01201	
22	2	0	1	2.436212	1.540500	36.86255			
23	-1	3	2 R	2.435718	2.434463	1.540500	36.87030	-0.01000	
24	-1	1	4	2.373534	1.540500	37.87250			
25	0	4	0	2.301011	1.540500	39.11395			
26	-2	2	1	2.294953	1.540500	39.22144			
27	2	2	0	2.275657	1.540500	39.54708			
28	-2	0	3	2.268354	1.540500	39.70053			
29	1	3	2	2.765078	1.540500	39.70457			
30	0	4	1	2.244153	1.540500	40.14697			
31	0	2	4	2.223398	1.540500	40.53812			
32	-2	2	2	2.203132	1.540500	40.92764			
33	2	0	2	2.179675	1.540500	41.33618			
34	-1	3	3 R	2.179295	2.178074	1.540500	41.35572	-0.02426	
35	2	2	1	2.153125	1.540500	41.97242			
36	0	4	2	2.095940	1.540500	43.12256			
37	1	1	4	2.038970	1.540500	43.27555			
38	-2	2	3	2.034620	1.540500	44.46051			
39	0	0	5	2.031553	1.540500	44.56125			
***	0	0	5	2.031553	2.030959	1.540500	44.56125	-0.01773	
40	-2	0	4	2.022424	1.540500	45.23316			
41	1	3	3 R	2.002753	2.002009	1.540500	45.23727	-0.01770	
42	2	2	2	1.969593	1.540500	46.07482			
43	-1	1	5	1.967715	1.540500	46.08671			
44	2	0	3	1.917904	1.540500	47.35776			
45	-1	3	4	1.917627	1.540500	47.36505			
46	0	4	1	1.903137	1.540500	47.74796			
47	0	2	5	1.895519	1.540500	48.96648			
48	-2	2	4	1.936523	1.540500	49.59427			
49	2	2	3	1.770320	1.540500	51.59215			
50	1	1	5	1.769035	1.540500	51.91006			
51	-2	0	5	1.757567	1.540500	51.97159			
52	1	3	4	1.757556	1.540500	51.97479			
53	-3	1	1	1.730973	1.540500	52.55313			
54	-2	4	1	1.736780	1.540500	52.65393			
55	1	5	0	1.736620	1.540500	52.65891			
56	2	4	0	1.728384	1.540500	52.92938			
57	-1	5	1	1.723225	1.540500	52.93476			
58	3	1	0	1.714911	1.540500	53.37814			
59	-3	1	2	1.714886	1.540500	53.37900			
60	0	4	4	1.705130	1.540500	53.70963			
61	-2	4	2	1.653946	1.540500	54.02325			
62	1	5	1	1.695618	1.540500	54.02765			
63	0	0	6	1.622361	1.540500	54.12128			
64	2	0	4	1.694012	1.540500	54.43759			
65	-1	3	5 R	1.643812	1.643801	1.540500	54.44458	54.4450	-0.00040
66	2	4	1	1.672616	1.540500	54.83240			
67	-1	5	2	1.672655	1.540500	54.93617			
68	-1	1	6	1.670334	1.540500	54.92081			
69	3	1	1	1.645554	1.540500	55.80316			
70	-3	1	3	1.645347	1.540500	55.80417			
71	-2	2	5	1.642226	1.540500	55.94241			
72	-2	4	3	1.611439	1.540500	56.55578			
73	1	5	2	1.615291	1.540500	56.95563			
74	0	2	6	1.622151	1.540500	57.99631			
75	-2	4	2	1.592420	1.540500	58.25494			
76	-1	6	3	1.592274	1.540500	58.26086			
77	2	2	4	1.541457	1.540500	59.2938F			
78	-2	0	6	1.544076	1.540500	59.67851			
79	1	3	5	1.544017	1.540500	59.67852			
80	3	1	2	1.547544	1.540500	59.6986P			
81	-3	1	4 R	1.547490	1.547484	1.540500	59.71139	59.72560	-0.02350
82	-3	3	1	1.534130	1.540500	60.2211C			
***	0	1	0	1.544076	1.534243	1.540500	60.2211F	60.27601	0.01119
83	0	1	0	1.534130	1.540500	60.2211P			
84	1	4	0	1.522274	1.540500	60.7744C			

NICKEL MICA MINUCIUS INDEXING

HKL LISTING - *** REFERS TO FIXED,R

R	H	K	L	D CALC	D OBS	LAMBDA	2-THETA CALC	2-THETA OBS	2-THETA DIFF
1	0	0	1	10.137272		1.540500	8.71529		
2	0	0	2	5.068634		1.540500	17.46152		
***	0	0	2	5.068634	5.074835	1.540500	17.46152	17.4600	0.02153
3	0	2	0	4.545019		1.540500	19.33885		
***	0	2	0	4.545019	4.584380	1.540500	19.33885	19.3450	-0.00612
4	1	1	0	4.550851		1.540500	19.53224		
5	-1	1	1	4.392442		1.540500	20.19897		
6	0	2	1	4.178190		1.540500	21.24649		
7	1	1	1	3.933608		1.540500	22.58438		
8	-1	1	2	3.660636		1.540500	24.29324		
***	1	1	-2	3.660636	3.658895	1.540500	24.29324	24.3050	-0.01174
9	0	2	2	3.600579		1.540500	26.18283		
10	0	0	3	3.379089		1.540500	26.35234		
***	0	0	3	3.379089	3.378128	1.540500	26.35234	26.3600	-0.00764
11	1	1	2	3.159820		1.540500	28.22668		
12	-1	1	3	2.925001		1.540500	30.53596		
***	1	1	-3	2.925001	2.924615	1.540500	30.53596	30.5400	-0.00413
13	0	2	3	2.720338		1.540500	32.89597		
14	-2	0	1	2.640466		1.540500	33.91406		
15	1	3	0	2.639385		1.540500	33.94162		
16	2	0	0	2.613174		1.540500	34.28586		
17	-1	3	1	2.608786	2.608074	1.540500	34.34534	34.3550	-0.00964
18	1	1	3	2.537777		1.540500	35.33759		
19	0	0	4	2.534316		1.540500	35.34736		
***	0	0	4	2.534316	2.534135	1.540500	35.36736	35.3900	-0.00262
20	1	3	1	2.502105		1.540500	35.85831		
21	-2	0	2	2.501787		1.540500	35.86301		
22	2	0	1	2.432746		1.540500	36.91696		
23	-1	3	2	2.427253	2.427477	1.540500	37.00290	37.0000	0.00290
24	-1	1	4	2.366239		1.540500	37.95374		
25	0	-4	0	2.292905		1.540500	39.25781		
26	-2	2	1	2.288582		1.540500	39.33508		
27	2	2	0	2.270426		1.540500	39.46128		
28	1	-3	2	2.262645		1.540500	39.80420		
29	-2	0	3	2.260506		1.540500	39.83682		
30	0	4	1	2.236415		1.540500	40.29190		
31	0	2	4	2.216130		1.540500	40.63664		
32	-2	2	2	2.196221		1.540500	41.06223		
33	2	0	2	2.177215		1.540500	41.4707		
34	-1	3	3	2.171935	2.172059	1.540500	41.54248	41.5400	0.00250
35	2	2	1	2.149070		1.540500	42.00525		
36	0	4	2	2.039095		1.540500	43.27094		
37	1	1	4	2.086105		1.540500	43.33609		
38	-2	2	3	2.027845		1.540500	44.464713		
39	0	0	5	2.027452		1.540500	44.65822		
40	1	3	3	1.598458		1.540500	45.33896		
41	-2	0	4	1.996211	1.996576	1.540500	45.39377	45.3850	0.00879
42	2	2	2	1.664904		1.540500	46.11133		
43	-1	1	5	1.961598		1.540500	46.23114		
44	2	0	3	1.915966		1.540500	47.40660		
45	-1	3	4	1.611434		1.540500	47.57289		
46	0	4	3	1.897339		1.540500	47.90302		
47	0	2	5	1.854311		1.540500	49.08691		
48	-2	2	4	1.630317		1.540500	49.77383		
49	2	2	3	1.767971		1.540500	51.65887		
50	1	1	5	1.757457		1.540500	51.97779		
51	1	3	4	1.754409		1.540500	52.08487		
52	-2	0	5	1.752143		1.540500	52.15729		
53	-3	1	1	1.735744		1.540500	52.68777		
54	-2	4	1	1.731404		1.540500	52.83005		
55	1	5	0	1.730818		1.540500	52.84933		
56	2	4	0	1.722503		1.540500	53.05113		
57	-1	5	1	1.722241		1.540500	53.13309		
58	1	1	0	1.711515		1.540500	53.49243		
59	-3	1	2	1.710179		1.540500	53.53757		
60	0	4	4	1.700289		1.540500	53.87408		
61	1	5	1	1.690458		1.540500	54.21295		
62	-2	4	-2	1.690361		1.540500	54.21634		
63	0	0	6	1.689545		1.540500	54.24466		
64	-2	0	4	1.682337		1.540500	54.49631		
65	-1	3	5	1.678635	1.678535	1.540500	54.62650	54.6300	-0.00348
66	2	4	1	1.668578		1.540500	54.95343		
67	-1	5	2	1.666815		1.540500	55.04654		
68	-1	1	6	1.665686		1.540500	55.0701		
69	3	1	1	1.643310		1.540500	55.90231		
70	-3	1	3	1.640946		1.540500	55.94990		
71	-2	2	5	1.636742		1.540500	56.14645		
72	1	5	2	1.610535		1.540500	57.14313		
73	-2	4	3	1.609858		1.540500	57.16797		
74	0	2	6	1.585365		1.540500	58.13623		
75	2	2	4	1.579410		1.540500	58.37668		
76	2	4	2	1.578840		1.540500	58.39978		
77	-1	5	3	1.576923		1.540500	58.4P175		
78	3	1	2	1.565543		1.540500	59.76879		
79	1	3	5	1.545115		1.540500	59.8C249		
80	2	0	4	1.542071		1.540500	59.00952		
81	-3	1	4	1.542491		1.540500	59.61464		
82	-3	3	1	1.530299		1.540500	60.44156		
83	0	6	0	1.529666		1.540500	60.51541		
84	2	6	5	1.529666	1.529730	1.540500	60.51541	60.5100	0.00543
85	3	2	0	1.514347		1.540500	60.34537		

COPPER MICA, RHM-M49, 700 C AND 2 KB, MONOCLINIC.

HAL LISTING - *+ REFERS TO FIXE.

N	I	K	L	U	V	W	U	V	W	LAMBDA	2-THETA CALC	2-THETA DRS	2-THETA DIFF
1	0	0	1	10.1611137	5.060568		1.540500			8.69477			
2	0	0	2	4.616814			1.540500			17.44012			
3	0	2	0	4.616814	4.617482		1.540500			19.20779			
4	1	1	0	4.562205			1.540500			19.43993			
4	1	1	0	4.562205	4.556385		1.540500			19.43993			
5	-1	1	1	4.416667			1.540500			20.08612			
6	0	2	1	4.203287			1.540500			21.11816			
7	1	1	1	3.946623			1.540500			22.50893			
8	-1	1	1	3.546623	3.546641		1.540500			22.50893			
8	-1	1	2	3.675562			1.540500			24.16373			
8	-1	1	2	3.675562	3.675774		1.540500			24.16373			
9	0	2	2	3.416150			1.540500			26.05635			
10	0	0	3	3.387C47			1.540500			26.28931			
10	0	0	3	3.387C47	3.383165		1.540500			26.28931			
11	1	1	2	3.166563			1.540500			28.15625			
12	-1	1	3	2.938649			1.540500			30.39061			
12	-1	1	3	2.938649	2.939652		1.540500			30.39061			
13	0	2	3	2.732942			1.540500			32.76462			
13	0	2	3	2.732942	2.730103		1.540500			32.7757			
14	1	3	0	2.6546E5			1.540500			33.73090			
15	-2	0	1	2.653650			1.540500			33.74710			
16	-1	2	1	2.625316			1.540500			34.12241			
17	2	0	0	2.623726			1.540500			34.14374			
17	2	0	0	2.623726	2.624379		1.540500			34.14374			
18	1	1	3	2.543058			1.540500			35.26169			
19	0	0	4	2.540264			1.540500			35.30148			
20	1	3	1	2.515513			1.540500			35.66074			
20	1	3	1	2.515513	2.513518		1.540500			35.66074			
21	-2	0	2	2.514810			1.540500			35.67102			
22	-1	3	2	2.442118			1.540500			36.77020			
22	-1	3	2	2.442118	2.443055		1.540500			36.79510			
23	2	0	1	2.44C521			1.540500			36.79510			
23	2	0	1	2.44C521	2.443055		1.540500			36.79510			
24	-1	1	4	2.376C75			1.540500			37.83047			
25	0	4	0	2.308C07			1.540500			38.98352			
26	-2	2	1	2.300E66			1.540500			39.11969			
27	2	2	0	2.2811C3			1.540500			39.46939			
28	1	2	2	2.272961			1.540500			39.61670			
29	-2	0	3	2.21265E			1.540500			39.62146			
30	0	4	1	2.2510C9			1.540500			40.01871			
31	0	2	4	2.225627			1.540500			40.49573			
32	-2	2	2	2.2C8434			1.540500			40.82498			
33	-1	3	3	2.1841C6			1.540500			41.30035			
34	2	0	2	2.182735			1.540500			41.32748			
34	2	0	2	2.182735	2.182861		1.540500			41.32748			
35	2	2	1	2.157E14			1.540500			41.83109			
36	0	4	2	2.101E44			1.540500			42.99969			
37	1	1	4	2.0501E3			1.540500			43.24771			
38	-2	2	3	2.039032			1.540500			44.38907			
39	0	5	5	2.032228			1.540500			44.54565			
39	0	5	5	2.032228	2.032690		1.540500			44.54565			
40	1	3	3	2.00C6195			1.540500			45.15533			
40	1	3	3	2.00C6195	2.007053		1.540500			45.15533			
41	-2	0	4	2.00C6195			1.540500			45.15549			
42	2	2	2	1.973311			1.540500			45.95050			
43	-1	1	5	1.969629			1.540500			46.04630			
44	-1	1	4	1.9211C3			1.540500			47.27408			
45	2	0	3	1.92017			1.540500			47.37243			
46	0	4	3	1.907516			1.540500			47.63153			
47	0	2	5	1.860C05			1.540500			48.92676			
48	-2	2	4	1.839580			1.540500			49.49478			
49	2	2	3	1.772822			1.540500			51.50397			
50	1	1	5	1.760E02			1.540500			51.88162			
51	-2	0	5	1.760398			1.540500			51.89444			
52	1	2	4	1.7602E2			1.540500			51.89813			
53	-3	1	1	1.743824			1.540500			52.425C2			
54	1	5	0	1.7415E8			1.540500			52.48416			
55	-2	4	1	1.741645			1.540500			52.49548			
56	-1	5	1	1.7335E4			1.540500			52.75912			
57	2	4	0	1.7331C8			1.540500			52.77411			
58	-3	1	2	1.7188E9			1.540500			53.24750			
59	2	1	0	1.7185E0			1.540500			53.25491			
60	0	4	4	1.7C8395			1.540500			53.59781			
61	1	5	1	1.7CC8C3			1.540500			53.85648			
62	-2	4	2	1.7C5CE5			1.540500			53.86392			
63	0	0	6	1.663522			1.540500			54.10684			
64	-1	3	5	1.6EE333			1.540500			54.35651			
65	2	0	4	1.685493			1.540500			54.38583			
65	2	0	4	1.685493	1.685516		1.540500			54.38583			
66	-1	5	2	1.677569			1.540500			54.66406			
67	2	4	1	1.677052			1.540500			54.68234			
68	-1	1	6	1.671575			1.540500			54.87656			
69	-3	1	3	1.649569			1.540500			55.67172			
70	3	1	1	1.649176			1.540500			55.68604			
71	-2	2	5	1.644E75			1.540500			55.84427			
72	1	5	2	1.619E13			1.540500			56.79379			
73	-2	4	3	1.619517			1.540500			56.79745			
74	0	2	6	1.589931			1.540500			57.95349			
75	-1	5	3	1.58E52C			1.540500			58.09000			
76	2	4	2	1.585595			1.540500			58.11108			
77	2	2	4	1.5C32C2			1.540500			58.22021			
78	-3	1	4	1.550E50			1.540500			59.56738			
79	3	1	2	1.5501E1			1.540500			59.58807			
80	-2	0	6	1.545511			1.540500			59.59863			
81	1	2	5	1.549150			1.540500			59.60547			
82	0	6	0	1.538E93			1.540500			60.05711			
82	0	6	0	1.538E93	1.5391C4		1.540500			60.06711			
83	-3	3	1	1.5384137			1.540500			60.10167			
84	0	4	5	1.5253349			1.540500			60.65823			
85	0	1	1	1.5253349			1.540500						

N.	h	k	l	D-GAT	D-BAS	I-4RDA	-2-TH-TA CALC	-2-TH-TA OBS	-2-TH-TA DIFF
1	0	0	1	10.188807		1.540500	8.67112		
2	0	0	2	5.6194603		1.540500	17.39240		
***	0	0	2	5.624603	5.793653	1.540500	17.39240	17.3950	-0.00259
3	0	2	0	4.620050		1.540500	19.19420		
***	0	2	0	4.620050	4.619864	1.540500	19.19420	19.1950	-0.00079
4	-1	1	0	4.570976		1.540500	19.40225		
***	1	1	0	4.570976	4.576180	1.540500	19.40225	19.3900	0.02227
5	-1	1	1	4.426703		1.540500	20.01364		
6	0	2	1	4.207685		1.540500	21.09584		
7	1	1	1	3.954204		1.540500	22.46521		
***	1	1	1	3.954204	3.953377	1.540500	22.46521	22.4700	-0.00477
8	-1	1	2	3.689365		1.540500	24.10123		
***	-1	1	2	3.689365	3.686538	1.540500	24.10123	24.1200	-0.01877
9	1	2	2	3.422113		1.540500	26.01364		
***	0	2	2	3.422113	3.420199	1.540500	26.01364	26.0300	-0.01635
10	0	3	3	3.396269		1.540500	26.21666		
***	0	3	3	3.396269	3.395209	1.540500	26.21666	26.2250	-0.00833
11	-1	1	2	3.173136		1.540500	28.09673		
***	1	1	2	3.173136	3.172775	1.540500	28.09673	28.1000	-0.00326
12	-1	1	3	2.946669		1.540500	30.30591		
***	-1	1	3	2.946669	2.948182	1.540500	30.30591	30.2900	0.01592
13	0	2	3	2.736443		1.540500	32.69693		
***	0	2	3	2.736443	2.737823	1.540500	32.69693	32.6800	0.01684
14	-2	0	1	2.460264		1.540500	33.66068		
15	1	3	0	2.657844		1.540500	33.69226		
16	2	0	0	2.629808		1.540500	34.06232		
***	2	0	0	2.629808	2.629612	1.540500	34.06232	34.0650	-0.00266
17	-1	2	1	2.628569		1.540500	34.07889		
18	1	1	2	2.549707		1.540500	35.18100		
19	0	0	4	2.547202		1.540500	35.20245		
***	0	0	4	2.547202	2.547377	1.540500	35.20245	35.2000	0.00247
20	-2	0	2	2.521552		1.540500	35.57245		
21	1	3	1	2.518521		1.540500	35.61670		
22	2	0	1,3	2.445632	2.447917	1.540500	36.71082	36.6800	0.03282
23	-1	3	2	2.445491		1.540500	36.71252		
24	-1	1	4	2.382730		1.540500	37.72079		
25	0	4	0	2.310025		1.540500	38.95514		
26	-2	2	1	2.305394		1.540500	39.03656		
27	2	0	0	2.285489		1.540500	39.39050		
28	-2	2	3,2	2.279117	2.278299	1.540500	39.55122	39.5200	-0.01477
29	1	3	2	2.276163		1.540500	39.55862		
30	0	4	1	2.252650		1.540500	39.98535		
31	0	2	4	2.230639		1.540500	40.40076		
32	-2	2	2	2.213352		1.540500	40.73022		
33	-1	3	3	2.188080		1.540500	41.22192		
34	0	0	2	2.187526		1.540500	41.23285		
35	1	2	1	2.161682		1.540500	41.74869		
36	0	4	2	2.133843		1.540500	42.95251		
37	1	1	4	2.09527		1.540500	43.14227		
38	-2	2	3	2.043944		1.540500	44.27673		
39	0	5	5	2.037762		1.540500	44.41824		
40	-2	0	4	2.012022	2.011912	1.540500	45.01740	45.0200	-0.00259
41	1	3	2	2.009498		1.540500	45.07706		
42	-2	2	2	1.977103		1.540500	45.85736		
43	-1	1	5	1.974997		1.540500	46.90906		
44	-1	3	4	1.925085		1.540500	47.17038		
45	2	0	3	1.924274		1.540500	47.19144		
46	0	4	3	1.910074		1.540500	47.56381		
47	0	2	5	1.954458		1.540500	48.80228		
48	-2	2	4	1.944683		1.540500	49.36017		
49	2	2	3	1.776356		1.540500	51.39407		
50	-2	0	5	1.765583		1.540500	51.73074		
51	1	1	5	1.765131		1.540500	51.74814		
52	1	3	4	1.763544		1.540500	51.79498		
53	-3	1	1	1.747952		1.540500	52.29178		
54	-2	-4	1	1.744213		1.540500	52.41245		
55	1	5	0	1.743528		1.540500	52.43457		
56	2	4	0	1.735544		1.540500	52.69431		
57	-1	5	1	1.735187		1.540500	52.70599		
58	-3	1	2	1.723094		1.540500	53.10471		
59	3	1	1	1.722475		1.540500	53.12531		
60	-2	4	-4	1.711154		1.540500	53.50458		
61	-2	4	2	1.703315		1.540500	53.77066		
62	1	5	1	1.702380		1.540500	53.82255		
63	2	0	6	1.698134		1.540500	53.94797		
64	-1	3	5	1.690141		1.540500	54.22397		
65	2	0	4	1.689301		1.540500	54.25317		
66	-2	-4	1	1.679427		1.540500	54.59854		
67	-1	5	2	1.679390		1.540500	54.59985		
68	-1	1	6	1.676312		1.540500	54.70847		
69	-3	1	3	1.653888		1.540500	55.51373		
70	3	1	1	1.652792		1.540500	55.65371		
71	-2	2	5	1.649254		1.540500	55.68326		
72	-2	4	3	1.622306		1.540500	56.68756		
73	1	5	2	1.621330		1.540500	56.72018		
74	0	2	6	1.593879		1.540500	57.79642		
75	-1	5	3	1.588568		1.540500	58.00800		
76	2	4	2	1.588356		1.540500	58.01645		
77	2	2	4	1.588568		1.540500	58.08017		
78	-3	1	4	1.554473		1.540500	59.29934		
79	-2	0	6	1.554494		1.540500	59.40521		
80	3	1	2	1.553510		1.540500	59.44669		
81	1	3	5	1.552877		1.540500	59.47336		
82	-1	2	1	1.551200		1.540500	59.49657		
83	1	6	0,2	1.540117	1.542131	1.540500	60.02772	59.9200	0.00073
84	1	6	0	1.540117		1.540500	60.02772		
85	1	6	5	1.540117		1.540500	60.51525		

ZINC MICA BMH-M101. NCT 100% MICA, BUT WELL XTALIZED. MONOCLINIC. HKL LISTING - *** REFERS TO FIXED, R

N	H	K	L	D CALC	D OBS	L AMRCA	2-THETA CALC	2-THETA OBS	2-THETA DIFF
1	0	0	1	10.151373		1.540500	8.70316		
2	C	C	2	5.075666		1.540500	17.45703		
***	0	0	2	5.075666	5.071955	1.540500	17.45703	17.4700	-0.01295
3	C	2	0	4.612772		1.540500	19.22478		
***	0	2	0	4.612772	4.609160	1.540500	19.22478	19.2401	-0.01521
4	1	1	0	4.560875		1.540500	19.44565		
***	1	1	0	4.560875	4.555171	1.540500	19.44565	19.4532	-0.00734
5	-1	1	1	4.416381		1.540500	20.08835		
6	0	2	1	4.199546		1.540500	21.13719		
7	1	1	1	3.944102		1.540500	22.52350		
8	-1	1	2	3.679170	3.676776	1.540500	24.16902		
***	-1	1	2	3.679170	3.676776	1.540500	24.16902	24.1850	-0.01597
9	C	2	2	3.413614		1.540500	26.08061		
10	0	0	3	3.383752	3.383802	1.540500	26.31505		
***	C	0	3	3.383752	3.383802	1.540500	26.31505	26.3150	0.00007
11	1	1	2	3.163815		1.540500	28.18121		
12	-1	1	3	2.937512		1.540500	30.40265		
13	C	2	3	2.728399		1.540500	32.79602		
14	-2	C	1	2.653656		1.540500	33.74435		
15	1	3	0	2.653C5		1.540500	33.75449		
16	-1	2	1	2.623126		1.540500	34.14374		
17	2	C	0	2.623456		1.540500	34.14734		
18	1	1	3	2.540575		1.540500	35.29727		
19	0	C	4	2.537843		1.540500	35.33655		
20	-2	C	2	2.515105		1.540500	35.66669		
21	1	2	1	2.513553		1.540500	35.68945		
22	-1	3	2	2.440650		1.540500	36.79248		
23	2	C	1	2.439654	2.438100	1.540500	36.80865	36.8330	-0.02432
24	-1	1	4	2.314837		1.540500	37.85092		
25	C	4	0	2.306366		1.540500	39.01910		
26	-2	2	1	2.300320		1.540500	39.12616		
27	2	-2	0	2.280437		1.540500	39.48141		
28	-2	C	3	2.2727E4		1.540500	39.61990		
29	1	3	2	2.27C98C		1.540500	39.65268		
***	1	3	2	2.27C980	2.27C3C6	1.540500	39.65268	39.6650	-0.01230
30	0	4	1	2.249C65		1.540500	40.05545		
31	0	2	4	2.223523		1.540500	40.53552		
32	-2	2	2	2.2C8151		1.540500	40.82968		
33	-1	2	3	2.1827E3		1.540500	41.32654		
***	2	C	2	2.181458	2.182609	1.540500	41.35278	41.3300	0.02280
34	2	0	2	2.181458		1.540500	41.35278		
35	2	2	1	2.156602		1.540500	41.85165		
36	C	4	2	2.055772		1.540500	43.01992		
37	1	1	4	2.088031		1.540500	43.29413		
38	-2	2	3	2.038746		1.540500	44.39563		
39	C	5	5	2.030214		1.540500	44.59082		
40	-2	C	4	2.0C6CCS		1.540500	45.15979		
41	1	2	3	2.0C4314		1.540500	45.20064		
***	1	3	3	2.0C4314	2.0C4548	1.540500	45.20064	45.1850	0.01505
42	2	2	2	1.972C52		1.540500	45.98157		
43	-1	1	5	1.968215		1.540500	46.07626		
44	-1	3	4	1.919868		1.540500	47.30637		
45	2	C	3	1.918568		1.540500	47.34036		
46	0	4	3	1.905754		1.540500	47.67728		
47	C	2	5	1.858244		1.540500	48.97620		
48	-2	2	4	1.835584		1.540500	49.59616		
49	2	2	3	1.771452		1.540500	51.54675		
50	-2	C	5	1.760011		1.540500	51.92671		
51	1	1	5	1.75E574		1.540500	51.93958		
52	1	3	4	1.758555		1.540500	51.95273		
53	-3	1	1	1.743824		1.540500	52.42502		
54	-2	4	1	1.74C835		1.540500	52.52173		
55	1	5	0	1.740621		1.540500	52.52884		
56	-1	5	1	1.732251		1.540500	52.80222		
57	2	4	0	1.732174		1.540500	52.80475		
58	-3	1	2	1.718937		1.540500	53.24326		
59	3	1	0	1.718365		1.540500	53.26239		
60	0	4	4	1.706837		1.540500	53.65082		
61	-2	4	2	1.655866		1.540500	53.88849		
62	1	5	1	1.655385		1.540500	53.90494		
63	0	6	6	1.651855		1.540500	54.16315		
64	-1	2	5	1.665179		1.540500	54.39679		
65	2	C	4	1.664031	1.683944	1.540500	54.43695		
***	2	0	4	1.684031	1.683944	1.540500	54.43695	54.4400	-0.00302
66	-1	2	2	1.676331		1.540500	54.70782		
67	2	4	1	1.675556		1.540500	54.71967		
68	-1	1	6	1.670435		1.540500	54.91702		
69	-3	1	3	1.6495111		1.540500	55.66647		
70	3	1	1	1.646E701		1.540500	55.70358		
71	-2	2	5	1.644381		1.540500	55.86270		
72	-2	4	3	1.6188E1		1.540500	56.82294		
73	1	5	2	1.61819E		1.540500	56.84793		
74	C	2	6	1.58842C		1.540500	58.01389		
75	-1	5	3	1.585357		1.540500	58.13669		
76	2	4	2	1.584E49		1.540500	58.15710		
77	2	2	4	1.5819C6		1.540500	58.27570		
78	-3	1	4	1.550722		1.540500	59.56433		
***	3	1	-4	1.550722	1.550542	1.540500	59.56433	59.5550	0.00334
79	3	1	2	1.5494E4		1.540500	59.61758		
80	-2	C	6	1.549357		1.540500	59.62042		
81	1	3	5	1.54819E		1.540500	59.67133		
82	-3	3	1	1.537E37		1.540500	60.11459		
83	C	6	0	1.537591		1.540500	60.12521		
***	C	6	0	1.537591	1.537711	1.540500	60.12521	60.1200	0.01522
E4	C	4	5	1.523940		1.540500	60.72025		
F5	-3	?	2	1.5206F7		1.540500	60.86386		

MR MICA RHM-MSI. NOT LOGG, BUT GOLD PATTERN. MONOCLINIC.

HKL LISTING - *** REFERS TO FIXED

N	H	K	L	D CALC	D OBS	LAMRCA	2-THETA CALC	2-THETA OBS	2-THETA DIFF
1	-	0	1	10.156191		1.540500	6.69902		
2	-	0	2	5.078C55		1.540500	17.44868		
***	0	0	2	5.078C55	5.105662	1.540500	17.44868	17.3400	0.10869
3	0	2	0	4.683037		1.540500	18.93364		
***	0	2	0	4.683C37	4.595688	1.540500	18.93364	19.2800	-0.34635
4	1	1	0	4.535025		1.540500	19.55756		
***	1	1	0	4.535029	4.531028	1.540500	19.55756	19.5750	-0.01144
5	-1	1	1	4.442572		1.540500	19.96689		
6	0	2	1	4.252714		1.540500	20.86995		
7	1	1	1	3.853166		1.540500	22.82201		
8	-1	1	2	3.724612		1.540500	23.86977		
***	-1	1	2	3.724612	3.723043	1.540500	23.86977	23.8300	-0.01122
9	0	2	2	3.442612		1.540500	25.85757		
10	0	0	3	3.385357		1.540500	26.30235		
***	0	0	3	3.385357	3.386961	1.540500	26.30235	26.2900	0.01237
11	1	1	2	3.120126		1.540500	28.58411		
***	1	1	2	3.120129	3.170012	1.540500	28.58411	28.1250	0.45912
12	-1	1	3	2.976154		1.540500	29.99857		
13	0	2	3	2.7435E1		1.540500	32.60947		
***	0	2	3	2.7435E1	2.744769	1.540500	32.60947	32.5950	0.01450
14	1	3	0	2.674347		1.540500	33.47821		
15	-1	3	1	2.6550E7		1.540500	33.72827		
16	-2	0	1	2.641927		1.540500	33.90121		
***	-2	0	1	2.641937	2.642788	1.540500	33.90121	33.8900	0.01123
***	2	0	0	2.551567	2.621025	1.540500	34.58066	34.1800	0.40067
17	2	0	0	2.591567		1.540500	34.58066		
18	0	0	4	2.539C41		1.540500	35.31924		
19	-2	0	2	2.523481		1.540500	35.54434		
20	1	2	1	2.522388		1.540500	35.56027		
21	1	1	3	2.5C9010		1.540500	35.75626		
22	-1	2	2	2.474766		1.540500	36.26813		
***	2	0	1	R 2.397964	2.456326	1.540500	37.47220	36.5500	0.92221
23	-1	1	4	2.403518		1.540500	37.38242		
24	2	0	1	2.397564		1.540500	37.47220		
25	0	4	0	2.341518		1.540500	38.41049		
26	-2	2	1	2.301023		1.540500	39.11371		
27	-2	0	3	2.292558		1.540500	39.25623		
28	0	4	1	2.281665		1.540500	39.45929		
29	1	3	2	2.27C617		1.540500	39.65457		
30	2	2	0	2.2671515		1.540500	39.71582		
31	0	2	4	2.2320E5		1.540500	40.37344		
32	-2	2	2	2.2214E1		1.540500	40.57452		
33	-1	3	3	2.213525		1.540500	40.72693		
***	2	0	2	R 2.140250	2.178827	1.540500	42.18661	41.4050	0.78162
34	2	0	2	2.140250		1.540500	42.18661		
35	2	2	1	2.134416		1.540500	42.30743		
36	0	4	2	2.126357		1.540500	42.47552		
37	1	1	4	2.0655E8		1.540500	43.79867		
38	-2	2	3	2.059384		1.540500	43.92743		
39	C	0	5	2.031239		1.540500	44.56851		
***	0	0	5	2.031239	2.029015	1.540500	44.56851	44.6200	-0.05162
40	-2	0	4	2.0296E8		1.540500	44.67416		
41	1	3	3	1.9998E5		1.540500	45.30762		
***	1	3	3	1.9998C5	1.9997C6	1.540500	45.30762	45.3100	-0.00239
42	-1	1	5	1.989258		1.540500	45.56036		
43	2	2	2	1.946553		1.540500	46.61816		
44	-1	3	4	1.945147		1.540500	46.65491		
45	0	4	3	1.925765		1.540500	47.15259		
46	2	0	3	1.882772		1.540500	48.29709		
47	0	2	5	1.863455		1.540500	48.82916		
48	-2	2	4	1.8623C6		1.540500	48.86237		
49	-2	0	5	1.782668		1.540500	51.19988		
50	1	5	0	1.761654		1.540500	51.85342		
51	-1	5	1	1.756154		1.540500	52.02924		
52	1	2	4	1.752577		1.540500	52.14340		
53	-2	4	1	1.752334		1.540500	52.15118		
54	2	2	3	1.7468E0		1.540500	52.32632		
55	1	1	5	1.742655		1.540500	52.46271		
56	2	4	0	1.73735E		1.540500	52.63376		
57	-3	1	1	1.7325E7		1.540500	52.79120		
58	C	4	4	1.7213C6		1.540500	53.16422		
59	-3	1	2	1.716520		1.540500	53.31076		
60	-2	4	2	1.716431		1.540500	53.32715		
61	1	5	1	1.716C66		1.540500	53.33868		
62	-1	2	5	1.705251		1.540500	53.70468		
63	-1	5	2	1.700E55		1.540500	53.85455		
64	3	1	0	1.699C46		1.540500	53.91666		
65	0	0	6	1.692658		1.540500	54.13531		
66	-1	1	6	1.68E2E4		1.540500	54.35889		
***	2	0	4	R 1.654572	1.665E5E	1.540500	54.48880	54.3900	1.10983
67	2	4	1	1.6753C4		1.540500	54.74417		
68	-2	2	5	1.666041		1.540500	55.07425		
69	-3	1	3	1.655822		1.540500	55.44333		
70	2	0	4	1.654572		1.540500	55.48880		
71	-2	4	3	1.6382E0		1.540500	56.08905		
72	1	5	2	1.630155		1.540500	56.39355		
73	3	1	1	1.624179		1.540500	56.61969		
74	-1	5	3	1.608544		1.540500	57.22052		
75	0	2	6	1.5919C0		1.540500	57.87503		
76	2	4	2	1.579157		1.540500	58.36261		
77	-2	0	6	1.569417		1.540500	58.78467		
78	-3	1	4	1.562467		1.540500	59.07199		
79	0	6	0	1.561012		1.540500	59.13248		
80	2	2	4	1.560C64		1.540500	59.17203		
81	0	6	1	1.542E54		1.540500	59.89734		
82	1	3	5	1.542147		1.540500	59.92935		
***	0	6	0	R 1.561012	1.5734934	1.540500	59.13248	60.2400	-1.10751
E3	-3	2	1	1.535153		1.540500	60.23953		
E4	C	4	5	1.5343E1		1.540500	60.26483		
E5	-2	4	4	1.534367		1.540500	60.29364		

RUBIN PHLOGOPITE PHM-N12R, T = 7200 AND P = 2KPa, MONOCLINIC

HKL LISTING - *** REFERS TO TABLE

N	H	K	L	D-GALC	D-SAS	I	ANALOG	2-THETA-GALC	2-THETA-OBS	2-THETA-DIFF
1	1	0	1	10.130481	1.540500	1	8.72079			
2	1	0	2	5.065442	1.540500	1	17.49261			
***	2	2	2	5.065442	5.066198	1	17.49261	17.4900	17.49263	
3	0	2	0	4.588264	1.540500	1	19.32845			
***	2	2	0	4.588264	4.584380	1	19.32845	19.3450	19.31653	
4	1	1	0	4.544901	1.540500	1	19.91466			
5	-1	1	1	4.363264	1.540500	1	20.33548			
6	0	2	1	4.170591	1.540500	1	21.23929			
7	1	1	1	3.959539	1.540500	1	22.43454			
***	1	1	1	3.959539	3.885965	1	22.43454	22.8650	22.43044	
8	-1	1	2	3.624147	1.540500	1	24.54025			
9	0	2	2	3.402610	3.512426	1	26.18259	25.3350	26.84760	
***	1	2	2	3.402610	3.408618	1	26.18259	26.1200	26.36260	
10	0	3	3	3.376962	1.540500	1	26.36923			
***	1	3	3	3.376962	3.376238	1	26.36923	26.3750	26.33576	
11	1	-1	2	3.183963	1.540500	1	27.99922			
12	-1	1	3	2.896240	1.540500	1	30.84659			
13	-2	2	-2	2.714727	2.766659	1	32.90444	32.3300	32.57346	
14	1	3	0	2.647612	1.540500	1	33.91876			
15	-2	2	-1	2.629469	2.624751	1	34.06686	34.1300	34.76311	
16	2	3	0	2.615809	1.540500	1	34.25021			
***	2	2	0	2.615809	2.615828	1	34.25021	34.2500	34.00021	
17	-1	3	1	2.603528	1.540500	1	34.41684			
18	-1	1	-3	2.556653	1.540500	1	35.06812			
19	2	1	4	2.532721	1.540500	1	35.41040			
***	0	0	4	2.532721	2.532749	1	35.41040	35.4100	35.00043	
20	1	3	1	2.509540	2.509436	1	35.74844	35.7500	35.00156	
21	-2	1	2	2.479900	1.540500	1	36.1943			
22	2	3	1	2.445968	2.455675	1	36.7127	36.5600	36.15027	
23	-1	3	-2	2.412339	1.540500	1	37.16083			
24	-1	1	4	2.345395	1.540500	1	38.34451			
25	0	-4	0	2.294131	1.540500	1	39.23602			
26	-2	2	1	2.281388	1.540500	1	39.46426			
27	-1	-3	2	2.272466	1.540500	1	39.62570			
28	2	?	1	2.272450	2.265645	1	39.62598	39.7500	39.12472	
29	1	-4	1	2.232481	1.540500	1	40.27188			
30	-2	1	3	2.235716	1.540500	1	40.30502			
31	0	2	4	2.217336	1.540500	1	40.65384			
32	2	2	2	2.196574	1.540500	1	41.09442			
33	-2	2	-2	2.181633	1.540500	1	41.34930			
34	-1	3	3	2.160593	1.540500	1	41.77072			
35	-2	2	-1	2.154423	1.540500	1	41.81467			
36	1	1	4	2.099712	1.540500	1	43.04120			
37	0	4	2	2.089795	1.540500	1	43.25571			
38	0	1	5	2.026176	2.026429	1	44.68588	44.6800	44.00589	
39	-2	2	-3	2.009816	1.540500	1	45.64952			
40	1	3	3	2.008990	1.540500	1	45.11041			
41	2	2	2	1.924270	1.540500	1	45.79208			
42	-2	1	4	1.972543	1.540500	1	45.96945			
43	-1	-1	5	1.946800	1.540500	1	46.61292			
44	2	0	3	1.933081	1.540500	1	46.96353			
45	-1	-3	4	1.900745	1.540500	1	47.81180			
46	0	4	3	1.897654	1.540500	1	47.89456			
47	0	2	-5	1.853496	1.540500	1	49.10492			
48	-2	2	4	1.812173	1.540500	1	50.30667			
49	2	2	3	1.781432	1.540500	1	51.23770			
50	1	1	5	1.767385	1.540500	1	51.67407			
51	1	-3	4	1.762757	1.540500	1	51.81982			
52	1	5	0	1.731831	1.540500	1	52.81601			
53	-2	0	5	1.731772	1.540500	1	52.81793			
54	-3	1	1	1.731460	1.540500	1	52.82822			
55	-2	-4	1	1.728676	1.540500	1	52.91989			
56	2	6	0	1.724778	1.540500	1	53.04880			
57	-1	-5	1	1.721243	1.540500	1	53.16629			
58	3	1	0	1.713213	1.540500	1	53.43524			
59	0	-6	4	1.708305	1.540500	1	53.87350			
60	-3	1	2	1.702286	1.540500	1	53.87418			
61	2	0	4	1.697431	1.540500	1	53.97214			
62	1	5	1	1.693238	1.540500	1	54.11667			
63	3	-3	6	1.686480	1.688385	1	54.28168	54.2850	54.00330	
64	-2	4	2	1.686405	1.540500	1	54.43643			
65	2	4	-1	1.673301	1.540500	1	54.81519			
66	-1	3	5	1.669331	1.540500	1	54.95657			
67	-1	-5	2	1.664048	1.540500	1	55.14584			
68	-1	1	6	1.654311	1.540500	1	55.49829			
69	3	-1	-1	1.646496	1.540500	1	55.65787			
70	-3	1	3	1.627071	1.540500	1	56.50998			
71	-2	2	5	1.602040	1.540500	1	56.77103			
72	1	5	2	1.614482	1.540500	1	56.99375			
73	-2	4	3	1.601144	1.540500	1	57.50958			
74	2	2	4	1.591981	1.540500	1	57.87183			
75	-2	-4	2	1.585827	1.540500	1	58.11783			
76	0	2	6	1.584590	1.540500	1	58.16751			
77	-1	5	3	1.572862	1.540500	1	58.64397			
78	3	1	2	1.555208	1.540500	1	59.37527			
79	1	-3	5	1.552039	1.540500	1	59.50870			
80	3	6	0	1.529422	1.529531	1	60.47977			
81	-3	3	1	1.527540	1.540500	1	60.56207			
82	-3	3	4	1.526671	1.540500	1	60.60016			
83	-2	1	6	1.526123	1.540500	1	60.62421			
84	1	-1	6	1.519794	1.540500	1	60.90344			
85	2	4	5	1.518465	1.540500	1	60.95349			
86	3	3	0	1.514967	1.540500	1	61.11819			
87	2	6	1	1.512286	1.540500	1	61.23116			
88	1	-5	4	1.513945	1.511020	1	61.29565	61.2950	60.00067	
89	-3	3	2	1.516776	1.540500	1	61.52118			
90	2	2	5	1.497355	1.540500	1	61.91568			
91	-2	4	4	1.494585	1.540500	1	61.99243			

GALIUM PHLOGOPITE PHM-4199. T = 720°C AND P = 2kPa MONOCLINIC. XML LISTING - *** REFERS TO FIXED.

N	H	K	L	D-GALC	D-BRS	A-4440A	2-THETA-GALC	2-THETA-BRS	2-THETA-DIF
1	9	0	1	10.207149	10.266955	1.540500	8.65551		
**	1	1	1	1 R 10.207149	10.266955	1.540500	8.65551	8.6050	0.05051
2	0	0	2	5.103574		1.540500	17.36090		
**	1	0	2	5.103574	5.111147	1.540500	17.36090	17.3350	0.02591
3	0	2	0	4.608973		1.540500	19.24078		
**	1	2	0	4.608973	4.608973	1.540500	16.24078	19.2400	-0.00079
4	1	1	0	4.561342		1.540500	19.44363		
**	1	1	0	4.561342	4.566840	1.540500	19.44363	19.4200	0.02364
5	-1	1	1 R	4.415116	4.425837	1.540500	20.09416	20.0450	0.04918
6	-1	2	1	4.201593		1.540500	21.13187		
7	1	1	1	3.952124		1.540500	22.47719		
**	1	1	1	3.952124	3.955083	1.540500	22.47719	22.4550	-0.02221
8	-1	1	2	3.642234		1.540500	24.14528		
**	-1	1	2	3.642234	3.6483527	1.540500	24.14528	24.1400	0.00528
9	0	2	2	3.425568		1.540500	26.02713		
10	3	-3	3	3.402384		1.540500	26.16870		
**	0	3	3	3.402304	3.402858	1.540500	26.16870	26.1650	0.00371
11	-1	1	2	3.175423		1.540500	28.07647		
**	1	1	2	3.175323	3.173328	1.540500	28.07647	28.0950	-0.0181
12	-1	1	3	2.944212		1.540500	30.33180		
**	-1	1	3	2.944212	2.944385	1.540500	30.33180	30.3300	0.00182
13	0	2	3	2.737323		1.540500	32.68610		
**	0	2	3	2.737323	2.736692	1.540500	32.68610	32.6950	-0.00888
14	-2	0	1	2.653230		1.540500	33.75262		
**	-2	1	1	2.653230	2.652667	1.540500	33.75262	33.7600	-0.00735
15	1	3	0 R	2.651731	2.645061	1.540500	33.77225	33.8600	-0.08774
16	2	0	0	2.624513		1.540500	34.13318		
**	2	0	0	2.624513	2.624005	1.540500	34.13318	34.1400	-0.00681
17	-1	3	1	2.622063		1.540500	34.16605		
18	-1	1	3	2.552144		1.540500	35.13246		
19	0	1	4	2.551787		1.540500	35.13715		
**	1	0	4	2.551787	2.551589	1.540500	35.13715	35.1400	-0.00284
20	-2	2	2 R	2.514787	2.514881	1.540500	35.67136	35.6700	0.01137
21	1	-3	1 R	2.514391	2.482249	1.540500	35.67719	36.1550	-0.47781
22	2	0	1	2.443385		1.540500	36.75043		
**	-1	3	2 R	2.442401	2.441940	1.540500	36.79385	36.7730	0.02287
24	-1	1	4	2.382398		1.540500	37.72641		
25	0	4	0	2.394486		1.540500	39.05255		
26	-2	2	1	2.299439		1.540500	39.14175		
27	2	2	0	2.286671		1.540500	39.47720		
28	1	3	2 R	2.276913	2.274267	1.540500	39.59216	39.5930	-0.00182
29	-2	0	3	2.273952		1.540500	39.59869		
30	0	4	1	2.2747908		1.540500	40.07706		
31	2	2	4	2.232461		1.540500	40.36636		
32	-2	2	2	2.207559		1.540500	40.84189		
33	2	-3	2	2.187294		1.540500	41.23743		
34	-1	3	3	2.194718		1.540500	41.28824		
35	-2	2	1	2.158748		1.540500	41.80728		
36	0	4	2	2.177296		1.540500	43.72866		
37	-1	-1	4 R	2.108496	2.098376	1.540500	43.06741	43.0700	-0.00256
38	2	1	5	2.041430		1.540500	44.33417	44.3350	-0.00182
**	1	3	6	2.041430	2.041394	1.540500	44.33417	44.3350	-0.00182
39	-2	2	3	2.039261		1.540500	44.38395		
40	-1	3	3	2.009432		1.540500	45.08099		
41	-2	1	4 R	2.022635	2.0208740	1.540500	45.09747	45.0950	0.00250
42	2	2	2	1.976662		1.540500	45.88296		
43	-1	1	5	1.975515		1.540500	45.89386		
44	2	3	3	1.925650		1.540500	47.16689		
45	-1	3	4	1.923298		1.540500	47.21686		
46	0	4	3	1.904922		1.540500	47.61819		
47	0	0	5	1.866533		1.540500	48.74451		
48	-2	2	4	1.841967		1.540500	49.45535		
49	2	2	3	1.776649		1.540500	51.38495		
50	1	1	5	1.768241		1.540500	51.64725		
51	1	3	4	1.764372		1.540500	51.76889		
52	-2	3	5 R	1.742596	1.743449	1.540500	51.79337	51.7980	-0.00461
53	-3	1	1	1.743597		1.540500	52.43234		
54	-2	4	1 R	1.739844	1.740124	1.540500	52.55408	52.5450	0.00909
55	1	5	0	1.739422		1.540500	52.56784		
56	2	4	0	1.731672		1.540500	52.82123		
57	-1	5	1	1.730968		1.540500	52.84439		
58	-3	1	0	1.714284		1.540500	53.24170		
59	-3	1	2	1.718420		1.540500	53.26053		
60	1	4	4	1.710283		1.540500	53.53406		
61	2	0	6	1.701191		1.540500	53.84317		
62	-2	4	2	1.699129		1.540500	53.91794		
63	1	5	1	1.698887		1.540500	53.92215		
64	-2	0	4	1.649166		1.540500	54.18039		
65	-1	3	5	1.689440	1.689304	1.540500	54.24832	54.2530	-0.00467
66	-1	1	6	1.677351		1.540500	54.67175		
67	2	4	1	1.676473		1.540500	54.70279		
68	-1	5	2	1.675577		1.540500	54.73465		
69	3	1	1	1.650461		1.540500	55.63898		
70	-3	1	2	1.649446		1.540500	55.67554		
71	-2	2	5	1.647129		1.540500	55.76135		
72	1	5	2	1.618745		1.540500	56.82700		
73	-2	4	3	1.618614		1.540500	56.83200		
74	2	2	6	1.595947		1.540500	57.71442		
75	2	2	4	1.587662		1.540500	58.04422		
76	-2	4	2 R	1.586464	1.586329	1.540500	58.09225	58.0980	-0.00574
77	-1	5	3	1.585480		1.540500	58.13177		
78	1	3	5	1.554214		1.540500	59.41705		
79	-2	0	6 R	1.553476	1.552957	1.540500	59.44812	59.4700	-0.02185
80	3	1	2	1.552330		1.540500	59.49643		
81	-1	1	4	1.551047		1.540500	59.54892		
82	-3	1	1	1.537460		1.540500	60.13342		
83	2	4	0	1.536325		1.540500	60.17987		
84	1	4	4	1.528098		1.540500	60.53812		
85	1	1	6	1.521955		1.540500	60.61219		

FFRRR1-PH153721TF 4MH-M111, T = 490C AND 2% MONOCHLORIC.

HKL LISTING - THE BARS TO FIX.

N	J	M	I	E-E _{ATC}	D-DBS	L-AMDA	R-THETA-GALC	P-THETA-DRS	S-THETA-DIFC
1	2	0	1	17.163512		1.540500	8.69094		
2	3	-2	2	5.042806		1.540500	17.43240		
3	3	2	2	5.182806	5.087847	1.540500	17.43240	17.4150	0.01741
4	0	2	n	4.638136	4.627028	1.540500	19.11865	19.1650	-0.04633
5	-1	1	1	4.438571		1.540500	19.98689		
6	-2	2	-1	4.219679		1.540500	21.03520		
7	1	1	1	3.963113		1.540500	22.41406		
8	-1	1	-1	3.963113	3.963824	1.540500	22.41406	22.4100	0.00407
9	-1	1	2	3.692713	3.696352	1.540500	24.07904	24.0550	-0.02406
10	0	2	2	3.426100	3.421492	1.540500	25.98438	26.0200	-0.03561
11	3	3	3	3.388538		1.540500	26.27753	26.2700	0.00755
12	-1	1	3	2.945463		1.540500	30.31862		
13	-1	1	3	2.945463	2.942016	1.540500	30.31862	30.3550	-0.03637
14	0	2	3	2.736120	2.735379	1.540500	32.73087	32.7100	-0.00912
15	-1	3	6	2.647786		1.540500	33.56296		
16	-2	1	1 R	2.668512	2.652286	1.540500	33.55356	33.7650	-0.21143
17	-2	0	0	2.638315		1.540500	33.94916		
18	2	0	0	2.638315	2.638254	1.540500	33.94916	33.9500	-0.00082
19	-1	-3	1	2.637713		1.540500	33.95715		
20	-2	0	-2	2.527308		1.540500	35.18692		
21	1	3	1	2.526681		1.540500	35.20549		
22	-2	0	-1 R	2.452557	2.485240	1.540500	36.60815	36.1100	0.49817
23	-1	3	2 R	2.452154	2.451144	1.540500	36.61435	36.6300	-0.01563
24	-1	3	2 R	2.452154	2.426212	1.540500	36.61435	37.0203	-0.40564
25	-3	4	0	2.319368		1.540500	37.76630		
26	-2	2	1	2.313708	2.313459	1.540500	38.90286	38.8950	0.03787
27	-2	2	0	2.293262		1.540500	39.25153		
28	-2	0	3	2.282026		1.540500	39.45276		
29	-1	3	2 R	2.281440	2.270299	1.540500	39.46935	39.5200	-0.05664
30	0	4	1	2.261982		1.540500	39.83545		
31	-3	2	-4	2.228758		1.540500	40.43634		
32	-2	2	2	2.219286		1.540500	40.61655		
33	-2	-3	2	2.191642		1.540500	41.15189		
34	-1	3	3	2.191414		1.540500	41.15637		
35	-2	2	1	2.168106		1.540500	41.61923		
36	0	4	2	2.129839		1.540500	42.82440		
37	-1	-1	4	2.093616		1.540500	43.17712		
38	-2	2	3	2.047606		1.540500	44.19339		
39	0	0	-5	2.033122		1.540500	44.52502		
40	-2	3	4	2.012706		1.540500	45.80128		
41	1	3	3 R	2.012259	2.012463	1.540500	45.81178	45.0070	0.00479
42	-2	2	-2	1.981557		1.540500	45.74844		
43	-1	1	5	1.971972		1.540500	45.98596		
44	-2	0	-3	1.926361		1.540500	47.13773		
45	-1	3	4	1.926226		1.540500	47.14072		
46	0	4	3	1.913788		1.540500	47.46588		
47	0	2	5	1.862080		1.540500	48.86868		
48	-2	2	4	1.844356		1.540500	49.31244		
49	2	2	3	1.779707		1.540500	51.31189		
50	-2	0	-5	1.764915		1.540500	51.75174		
51	1	3	4	1.764583		1.540500	51.76224		
52	1	1	5	1.763001		1.540500	51.81210		
53	-3	1	1	1.753640		1.540500	52.10941		
54	-2	4	-1	1.750429		1.540500	52.21219		
55	1	5	0 R	1.750223	1.750187	1.540500	52.21881	52.2200	-0.00116
56	-2	4	0	1.741823		1.540500	52.48981		
57	-1	5	1	1.741650		1.540500	52.49545		
58	-3	1	2	1.728145		1.540500	52.83744		
59	3	1	0	1.728087		1.540500	52.93933		
60	-3	4	4	1.713049		1.540500	53.44077		
61	-2	6	2	1.709737		1.540500	53.58636		
62	1	-5	1	1.7078519		1.540500	53.59375		
63	0	3	6	1.694269		1.540500	54.08105		
64	-2	0	4	1.689080		1.540500	54.22922		
65	-1	3	5 R	1.699939	1.689679	1.540500	54.23099	54.2400	-0.05902
66	-2	4	1	1.685045		1.540500	54.40146		
67	-1	5	2	1.684915		1.540500	54.40604		
68	-1	1	-6	1.673248		1.540500	54.81708		
69	-3	1	3	1.657320		1.540500	55.37149		
70	-3	1	1	1.657699		1.540500	55.37415		
71	-2	2	5	1.649528		1.540500	55.67319		
72	-2	4	-3	1.626257		1.540500	56.52881		
73	1	5	2	1.626362		1.540500	56.53687		
74	-2	4	-2	1.592869		1.540500	57.83649		
75	-1	5	3	1.592781		1.540500	57.84000		
76	-3	2	6	1.591415		1.540500	57.89435		
77	2	2	4	1.587968		1.540500	58.03599		
78	-2	1	4	1.557422		1.540500	59.271921		
79	3	1	2	1.557374		1.540500	59.28442		
80	-2	0	6	1.553105		1.540500	59.44371		
81	1	3	5	1.552858		1.540500	59.47415		
82	-3	3	1 R	1.546680	1.546681	1.540500	59.74564	59.7400	0.00562
83	1	5	0	1.546645	1.546645	1.540500	59.76282	59.7400	0.02283
84	0	6	n	1.546645		1.540500	59.76282		
85	3	5	n R	1.546645	1.529646	1.540500	59.76282	60.4702	-0.77115
86	-3	3	2	1.528880	1.528880	1.540500	60.52345		
87	2	2	2	1.528880	1.528880	1.540500	60.52345	60.4700	0.22211

GERMANIUM PHLOGOPITE. RMH-M6A AT 600C AND 2KH. MONOCLINIC. HKL LISTING - *** REFERS TO FIXED.

N	H	K	L	D CALC	D OBS	LAMRCA	2-THETA CALC	2-THETA OBS	2-THETA DIFF
1	0	0	1	10.440727		1.540500	8.46151		
2	C	C	2	5.220366		1.540500	16.96960		
***	C	C	2	5.226366	5.223304	1.540500	16.96960	16.9600	0.00962
3	C	2	0	4.689141		1.540500	18.90878		
4	1	1	0	4.626929		1.540500	19.19052		
***	1	1	0	4.626929	4.625833	1.540500	19.19052	19.1700	0.02053
5	-1	1	1	4.475566		1.540500	19.81821		
6	0	2	1	4.277537		1.540500	20.74750		
7	1	1	1	4.012979		1.540500	22.13200		
***	1	1	1	4.012979	4.009761	1.540500	22.13200	22.1500	-0.01799
8	-1	1	2	3.743870		1.540500	23.74519		
***	-1	1	2	3.743870	3.744680	1.540500	23.74519	23.7400	0.00521
9	0	2	2	3.488463		1.540500	25.51195		
10	0	C	3	3.480244		1.540500	25.57321		
***	0	0	3	3.480244	3.479339	1.540500	25.57321	25.5800	-0.00676
11	1	1	2	3.232604		1.540500	27.57127		
***	1	1	2	3.232404	3.230828	1.540500	27.57127	27.5850	-0.01371
12	-1	1	3	2.955866		1.540500	29.75594		
***	-1	1	3	2.955866	2.955962	1.540500	29.75594	29.7550	0.00096
13	C	2	3	2.794634		1.540500	31.99762		
14	1	3	0	2.653557		1.540500	33.22742		
15	-2	C	1	2.683756		1.540500	33.35739		
***	-2	C	1	2.683756	2.683162	1.540500	33.35739	33.3650	-0.00760
16	-1	3	1	2.664315		1.540500	33.60794		
17	2	C	0	2.655143		1.540500	33.72754		
18	C	4		2.610182		1.540500	34.32635		
***	C	0	4	2.610182	2.609916	1.540500	34.32635	34.3300	-0.00363
19	1	1	3	2.602306		1.540500	34.43350		
20	1	3	1	2.556052		1.540500	35.07605		
21	-2	C	2	2.546760		1.540500	35.20877		
22	-1	2	2	2.482203		1.540500	36.15567		
23	2	C	1	2.471541		1.540500	36.25940		
24	-1	1	4	2.430760		1.540500	36.94821		
25	C	4	0	2.344570		1.540500	38.35855		
26	-2	2	1	2.329244		1.540500	38.62091		
27	1	3	2	2.314551		1.540500	38.87589		
28	2	2	0	2.31C465		1.540500	38.94742		
29	-2	0	3	2.307160		1.540500	39.02546		
30	C	4	1	2.2876C1		1.540500	39.35263		
31	0	2	4	2.28C656		1.540500	39.47748		
32	-2	2	2	2.237584		1.540500	40.26242		
33	-1	3	3	2.224533		1.540500	40.51651		
34	2	C	2	2.219955		1.540500	40.62297		
35	2	2	1	2.189C55		1.540500	41.20273		
36	1	1	4	2.141897		1.540500	42.15262		
37	C	4	2	2.138766		1.540500	42.21722		
38	C	5		2.088145		1.540500	43.29163		
39	-2	2	3	2.070150		1.540500	43.68719		
40	1	3	3	2.047112		1.540500	44.20459		
***	C	C	5 R	2.088145	2.042270	1.540500	43.29163	44.3150	-1.02335
41	-2	C	4	2.041677		1.540500	44.32849		
42	-1	1	5	2.017255		1.540500	44.89182		
43	2	2	2	2.006490		1.540500	45.14038		
44	-1	3	4	1.96C354		1.540500	46.27081		
45	2	C	3	1.957565		1.540500	46.34158		
46	C	4	3	1.9444E4		1.540500	46.67175		
47	C	2	5	1.9C7555		1.540500	47.63055		
48	-2	2	4	1.871935		1.540500	48.59476		
49	2	2	3	1.8C6465		1.540500	50.47662		
50	1	1	5	1.8059C7		1.540500	50.49344		
51	1	3	4	1.795157		1.540500	50.69623		
52	-2	C	5	1.755249		1.540500	50.81445		
53	1	5	0	1.766576		1.540500	51.63675		
54	-2	4	1	1.7656C0		1.540500	51.72769		
55	-3	1	1	1.763033		1.540500	51.78586		
56	-1	5	1	1.76C111		1.540500	51.90353		
57	2	4	0	1.752456		1.540500	51.98773		
58	0	4	4	1.744231		1.540500	52.41163		
59	C	6		1.740121		1.540500	52.54507		
60	3	1	0	1.739366		1.540500	52.56900		
61	-3	1	2	1.738955		1.540500	52.58173		
62	1	5	1	1.727810		1.540500	52.94849		
63	-2	4	2	1.724918		1.540500	53.04416		
64	-1	3	5	1.723434		1.540500	53.09341		
65	2	0	4	1.721701		1.540500	53.15106		
***	2	0	4	1.721701	1.722034	1.540500	53.15106	53.1400	0.01108
66	-1	1	6	1.713639		1.540500	53.42090		
67	-1	5	2	1.70C4442		1.540500	53.73224		
68	2	4	1	1.702216		1.540500	53.80817		
69	-2	2	5	1.671657		1.540500	54.69913		
70	3	1	1	1.671375		1.540500	54.88364		
71	-3	1	3	1.670662		1.540500	54.92836		
72	1	5	2	1.647146		1.540500	55.76071		
73	-2	4	3	1.644476		1.540500	55.85916		
74	0	2	6	1.631411		1.540500	56.34625		
75	2	2	4	1.616202		1.540500	56.92453		
76	-1	5	3	1.613750		1.540500	57.01898		
77	2	4	2	1.612016		1.540500	57.09594		
78	1	3	5	1.585935		1.540500	58.11349		
79	-2	C	6	1.5831C5		1.540500	58.22714		
80	3	1	2	1.573744		1.540500	58.60730		
81	-3	1	4	1.572876		1.540500	58.64279		
82	0	6	0	1.563047		1.540500	59.04785		
83	0	4	5	1.559351		1.540500	59.20178		
***	0	6	0 R	1.559347	1.557559	1.540500	59.04785	59.2750	-0.22714
E4	-3	3	1	1.557210		1.540500	59.29129		
E5	1	1	6	1.554676		1.540500	59.38919		
E6	C	6	1	1.545E21		1.540500	59.77237		
E7	1	5	7	1.442778		1.540500	59.93399		

VITA

The author was born in Rockville Center, Long Island, New York on November 1, 1948. He graduated with high honors from Ridgewood High School, Ridgewood, New Jersey where he concentrated in science and music. He entered the Massachusetts Institute of Technology in September of 1966, and subsequently enrolled in the five-year Masters degree program in the Department of Earth and Planetary Sciences.

In addition to his scientific studies, the author has studied trumpet privately for four years with Andre Come of the Boston Symphony Orchestra. He has been principle trumpet of the M. I. T. Symphony Orchestra for five years, and has appeared as soloist with the M. I. T. Concert Band, Symphony Orchestra, and many other groups in more than a dozen states.

Among the author's academic awards are the Harvard Alumni Award (1965), the New Jersey Science Teachers' Award (1966), Outstanding Musician--New York State Music Festival (1966), and the Phi Sigma Kappa Foundation Award (1968). He is a member of Sigma Xi, Phi Lambda Upsilon, and Baton honorary societies.

Professional experience includes summer work with Isotopes, Inc. of Westwood, New Jersey (1968) and as field assistant for the United States Geological Survey (1970). Next year the author will continue his studies at Harvard University, and will receive for a second year a National Science Foundation Fellowship.

The author was married to Margaret Joan Hindle on August 9, 1969.